Dissertation

submitted to the

Combined Faculties for the

Natural Sciences and for Mathematics

of the

Ruperto-Carola University of Heidelberg, Germany

for the degree of

Doctor of Natural Sciences

Presented by

Diplom-Biologin Isabel Brachmann

born in Ulm, Germany

Oral examination: 28.01.2011

Imaging peripheral nerve outgrowth into the developing forelimb of the mouse embryo

Referees:

Prof. Dr. Hilmar Bading

Prof. Dr. Joachim Kirsch

Index

Summary

In order to establish a proper functioning nervous system, several guidance molecules provide signals to allow precise pathfinding and patterning of axons. Many proteins regulating axonal guidance have been identified and characterized successfully by the analysis of dissociated neurons *in vitro*. However, these cultures neither allowed to investigate adhesive interactions between the growth cones and the surrounding tissue nor to analyze the role of the membrane anchorage of the guidance molecules and the receptor complex compositions which can induce various cell responses. It is therefore important to manipulate nerve outgrowth *in situ* and to observe the effects in real time.

The aim of my thesis was to establish a slice culture system that allows us to follow the outgrowth of peripheral nerves into the developing forelimb of the mouse, and to validate this *ex situ* model by the analysis of slices prepared from mice lacking the gene encoding the chemorepulsive guidance molecule semaphorin3A.

The first experiments were performed using a mouse line expressing the enhanced green fluorescent protein (EGFP) from the gene locus *Mapt*, resulting in an ectopic EGFP expression in postmitotic neurons of the central and peripheral nervous system. The slice culture system proved to be suitable to reproduce endogenous forelimb innervation and to image spinal nerve outgrowth into the murine forelimb as it starts from embryonic day (E) 10.5. Analysing the specification of non-neural tissues (chondrogenesis and myogenesis) confirmed that they retained a developmentally normal morphology over the course of the culture, and employing assays for the quantification of cell death revealed a very low mortality rate of neural and non-neural cells.

To solve the imaging restrictions resulting of the weak GFP intensity at the nerve ends, we planned to improve the system by employing a mouse line that was expected to have a stronger GFP signal intensity specifically in the growth cone.

Furthermore, we wanted to analyse the limb innervation in a mouse line deficient for the guidance protein semaphorin3A. Applying our system, we could clearly confirm premature outgrowth and a strong defasciculation of spinal nerves in homozygous mutant embryos. Furthermore, with the aid of the EGFP expression we were able to detect cells that had not been previously reported for this mouse line. Characterising these cells by immunohistochemistry, two distinct populations, namely a sensory and a sympathetic lineage, were detected. These cells

were shown to be located ectopically dur to the absence of semaphorin3A, revealing also an impact of this guidance molecule on neural crest migration.

Our established slice culture system allows the observation and analysis of spinal nerve outgrowth as it occurs *in situ* and therefore provides a system to determine the effect of guidance molecules on axonal outgrowth *ex vivo.*

Zusammenfassung

Eine Vielzahl von Signalmolekülen ist für die räumlich und zeitlich aufeinander abgestimmte Entwicklung des Nervensystems verantwortlich. Zu diesen zählen die axonalen Wegweisermoleküle, die ein korrektes Auswachsen der neuronalen Fortsätze garantieren. Ihre Charakterisierung wurde sehr erfolgreich in primären Zellkulturen verfolgt, die allerdings Untersuchungen zu Interaktionen zwischen Wachstumskegeln bzw. Axonen und dem umliegenden Gewebe ausschließen. Wie Studien der letzten Jahre belegen, sind jedoch nicht nur spezifische Wegweisermoleküle für die Zielführung von Bedeutung, sondern auch ihr Zusammenspiel, die Art und Weise ihrer Membranverankerung bzw. ihrer Sekretion, sowie die Zusammensetzung von Rezeptorkomplexen in der Nervenzellmembran, die insgesamt sehr unterschiedliche Zellantworten induzieren können. Um den Einfluss dieser Faktoren während der Ontogenese möglichst originalgetreu untersuchen zu können, bedarf es eines Kultursystems, das die Darstellung der dynamischen Vorgänge und gegebenenfalls ihre Modifizierung erlaubt.

Unser Ziel war es, ein solches System zu erstellen und zu optimieren, um das Auswachsen peripherer Nerven *in situ* zu dokumentieren, und an diesem Modell anschließend unter Verwendung einer mutanten Mauslinie den Einfluss eines spezifischen Wegweisemoleküls, des Semaphorins3A, auf das Nervenzellwachstum zu testen.

Als Ausgangspunkt diente eine bereits charakterisierte Mauslinie, deren Nervenzellen ein grün-fluoreszierendes Protein (GFP) exprimieren, das sowohl im Zellkörper, als auch in den Fortsätzen vorliegt, und somit das gesamte entstehende Nervensystem markiert. Durch Kultur von Gewebeschnitten über einen Zeitraum von mehreren Tagen gelang es uns, die initialen Schritte zur Innervation der vorderen Extremität in ihrem räumlichen und zeitlichen Ablauf zu analysieren. Nach Optimierung des Modells konnten wir aufzeigen, dass das Wachstum der Spinalnerven in Zeitraum und Muster, ähnlich dem in einem sich normal entwickelnden Embryo folgt. Unsere Untersuchungen des umliegenden Gewebes (Knorpel und Muskulatur) bestätigten eine zeitabhängige, fortschreitende Spezifizierung und belegten damit die hohe Qualität unseres Schnittkultursystems. Die Intensität des GFP-Signals reichte jedoch nicht aus, um die Dynamik der feinsten Nervenenden während der Wegfindung bei höherer Auflösung deutlich zu erfassen. Die Verwendung einer bis dahin uncharakterisierten Mauslinie M22 mit einer erhöhten GFP-Expressionsrate führte zu einer deutlichen Verbesserung. Die Befunde an unserem M22-Kultursystem zeigen, dass nicht nur die initialen Schritte der Extremitäteninnervation

dokumentiert werden können, sondern auch der Effekt spezifischer Wegweisermoleküle auf das Auswachsen von Spinalnerven.

Am Beispiel einer mutanten Semaphorin3A-defizienten Mauslinie konnten wir in Time-lapse-Studien den Nachweis erbringen, dass das Fehlen dieses Moleküls zu einem verfrühten Auswachsen der Spinalnerven, sowie zu ihrer stärkeren Verzweigung und Plexusbildung in Kombination mit ihrer geringeren Bündelung im Bereich der vorderen Extremität führt. Mit dem Nachweis ektopischer Neuralleistenabkömmlinge entlang mehrerer inkorrekt auswachsender Nervenbündel konnten wir erstmalig den wesentlichen Einfluss von Semaphorin3A auf die Migration von sensorischen und sympathischen Neuralleistenvorläuferzellen dokumentieren.

Die beschriebene M22-Gewebeschnitt-Kultur ermöglicht über einen definierten Zeitraum Einblick in die Entwicklung des peripheren Nervensystems zu nehmen und beispielhaft detailliert das fortschreitende Auswachsen von Spinalnerven zu analysieren. Darüber hinaus kann die Wirkung von Wegweisermolekülen im Rahmen dieses Wachstumsprozesses exakt bestimmt, und damit unser Verständnis zur Genese spezifischer Phänotypen vertieft werden.

1. Introduction

1.1 The developing peripheral nervous system

The vertebrate nervous system is divided into the central nervous system (CNS) and the peripheral nervous system (PNS), which consists of cranial, spinal and autonomic nerves and their associated ganglia. The latter is formed from the neural crest, from epidermal placodes, and from axons growing from cell bodies in the CNS (Slack 2006). This introduction covers the development of the trunk neural crest cells and the spinal nerves, as well as some molecular mechanisms needed for the establishment of a proper functioning nervous system.

1.1.1 Neural crest

The neural crest (NC) is a discrete transient structure that exists during vertebrate embryogenesis, and which comprises a population of cells called the neural crest cells (Le Douarin 2009). Neural crest cell induction begins during gastrulation at the interface between the neural plate and the ectoderm. As neurulation occurs, the NC precursors are located in the neural folds from where they delaminate and emigrate to follow distinct pathways, differentiate and eventually cluster at their target regions to form distinct structures. The development proceeds in a rostrocaudal manner along the body axis (Le Douarin 2009).

Neural crest cells are multipotent and give rise to a wide variety of different cell types, ranging from neurons and glia of sensory, autonomic and enteric ganglia, to adrenal medullary secretory cells, smooth muscle cells, melanocytes, and bone and cartilage cells. Furthermore, the NC can regenerate after ablation, in such a way that residual neural tube cells and adjacent NC compensate for the missing tissue (Sauka-Spengler and Bronner-Fraser 2008).

According to the anatomical regions the crest and their characteristic derivatieves originates, it can be divided into four groups: the cranial, cardiac, trunk, and vagal and sacral neural crest (Gilbert 2010).

1.1.2 The trunk neural crest cells

The population of the trunk neural crest cells gives rise to melanocytes, Merkel cells, the dorsal root ganglia (DRGs), neurons and ganglia of the sympathetic nervous system, as well as norepinephrine- and epinephrine-producing cells of the adrenal medulla (Hall 2009).

1.1.3 Migration of the trunk neural crest cells

Neural crest cell migration in mouse has been difficult to analyse due to the *in utero* development and a lack of reliable markers compared to other model organisms like the chick. Nevertheless, studies using scanning electron microscopy or labeling NC cells before their delamination, allowed a detailed description of their migratory pathways already 15 years ago and revealed similarities to the migration occurring in the trunk region of avians (Erickson and Weston 1983; Serbedzija et al., 1990). In the trunk region of mouse embryos the first neural crest cells appear between embryonic day (E) 8.5 and E9.0 in the dorsal wedge, a cell-free space that is bordered by the dorsal neural tube, the somites and the epidermis (Erickson and Weston 1983; Serbedzija et al., 1990). Soon after their separation from the neural epithelium, some neural crest cells begin to migrate laterally over the side of the neural tube (Serbedzija et al., 1990). The neural crest cells of each body segment move together and reach the dorsal border of the somite as a common front. From there on neural crest cells at the level of the forelimb migrate along two major pathways: the ventral and the dorsolateral pathway (Serbedzija et al., 1990).

1.1.3.1 The ventral migratory pathway

The ventral pathway is characterized by two overlapping phases of migration (Serbedzija et al., 1990). After delamination the first neural crest cells migrate ventrally around the epithelial somites either in the intersomitic space along the blood vessels or between the somites and the neural tube (Serbedzija et al., 1990; Schwarz et al., 2009). These neural crest cells reach the dorsal aorta and become neurons and glia of the sympathetic ganglia as well as adrenal chromaffin cells (Serbedzija et al., 1990; Schwarz et al., 2009). A second phase of migration takes place between E9 and proceeds through E10 where some neural crest cells invade and pass the sclerotome while most of the neural crest cells invade the rostral sclerotome and remain there coalescing to form the sensory neurons and the glia of the DRGs as well as the Schwann cells of the ventral roots of the spinal nerves (Serbedzija et al., 1990).

1.1.3.2 The dorso-lateral pathway

Neural crest cells migrating between the epidermal ectoderm and the dermomyotome are considered to follow a dorsolateral pathway. The first cells undertaking this route are detected

from E8.5, which is again in contrast to chick development (Serbedzija et al., 1990; Gammill and Roffers-Agarwal 2010). These cells will differentiate into melanocytes.

1.1.4 Patterning and guidance of trunk neural crest cells

Temporal and spatial regulation of guidance cues are used to form peripheral ganglia and nerves in register with the somite-derived vertebrae (Gammill and Roffers-Agarwal 2010). Though originally described to be important for axon guidance, genetic studies in mice revealed an impact of guidance cues, also on neural crest development and guidance.

During establishment of the metameric body axis, the extracellular matrices of the sclerotome differ in the anterior and posterior region of each somite. Only the extracellular matrix of the anterior sclerotome is permissive for neural crest migration. This segmentation of each somite is achieved by specific expression of at least two repulsive molecules, the ephrinB2 (Wang and Anderson 1997) and Sema3F (Gammill et al., 2006), in the posterior sclerotome. Mutant mice for ephrinB2 display a disruption of the segmented migration of trunk neural crest cells (Wang and Anderson 1997; Davy and Soriano 2007). A similar phenotype is observed in neuropilin-2 and semaphorin3F (Sema3F) mutant mice, where neural crest cells lose their segmental migration pattern and instead migrate as a uniform sheet through the somites (Gammill et al., 2006). Interestingly, the distribution of Sema3F seems to be somehow related to the expression of ephrinB2, since ephrinB2 null mice showed a disturbed Sema3F distribution in the posterior sclerotome (Davy and Soriano 2007).

Further molecules have been shown to be expressed in the posterior sclerotome and to be involved in establishing a patterned migration: versican (Dutt et al., 2006; Dutt et al., 2006), collapsin-1 (Sema3A) (Eickholt et al., 1999), peanut agglutinin (PNA) and chondroitin-6-sulfate (Oakley and Tosney 1991; Oakley et al., 1994), F-spondin (Debby-Brafman et al., 1999), and collagen IX (Ring et al., 1996).

1.1.5 Spinal nerves

Spinal nerves originate as a pair from each trunk segment and are formed by dorsal and ventral roots, which are attached to the spinal cord. The dorsal roots are composed of sensory fibres, whose neurons are located in the dorsal root ganglia (DRGs) lateral to the spinal cord, while the ventral roots are formed by fibres from motor neurons which are located in the ventral

mantle layer of the neural tube. At the level of the forelimb the spinal nerves join to form a network called the brachial plexus (Slack 2006).

1.2 Development and innervation of the mouse forelimb

1.2.1 Tissue patterning in the developing forelimb

The murine forelimb becomes first visible at E9.5 (Fig. 1.1) as a protrusion from the embryonic flank, opposite to somites 7-13 (Milaire and Mulnard 1984). At the beginning of the forelimb development, the limb consists of a two component epidermis (basal ectodermal layer and pavement like layer of periderm), which overlies a vascularized homogeneous connective-tissue (Martin 1990). During the initiation of limb bud development (E10), a specialized epithelium called the apical ectodermal ridge (AER), forms at the dorsoventral interface of the limb bud ectoderm (Muneoka et al., 1989; Zeller et al., 2009). The AER is required for bud outgrowth which is accompanied by the laying down of structures along the proximodistal axis of the limb (Towers and Tickle 2009). The cartilaginous skeletal elements develop sequentially in a proximodistal direction, becoming detectable at E11.5 in the proximal core of the forelimb staining for cartilage glycosaminoglycans (Martin 1990). Muscles can be first detected at E13.5. However, immunohistochemical analysis revealed the first myogenic cells in the forelimb at E11.5. These cells originate from the dermomyotome adjacent to the neural tube and head towards the base of the forelimb around E10.5 (Martin 1990).

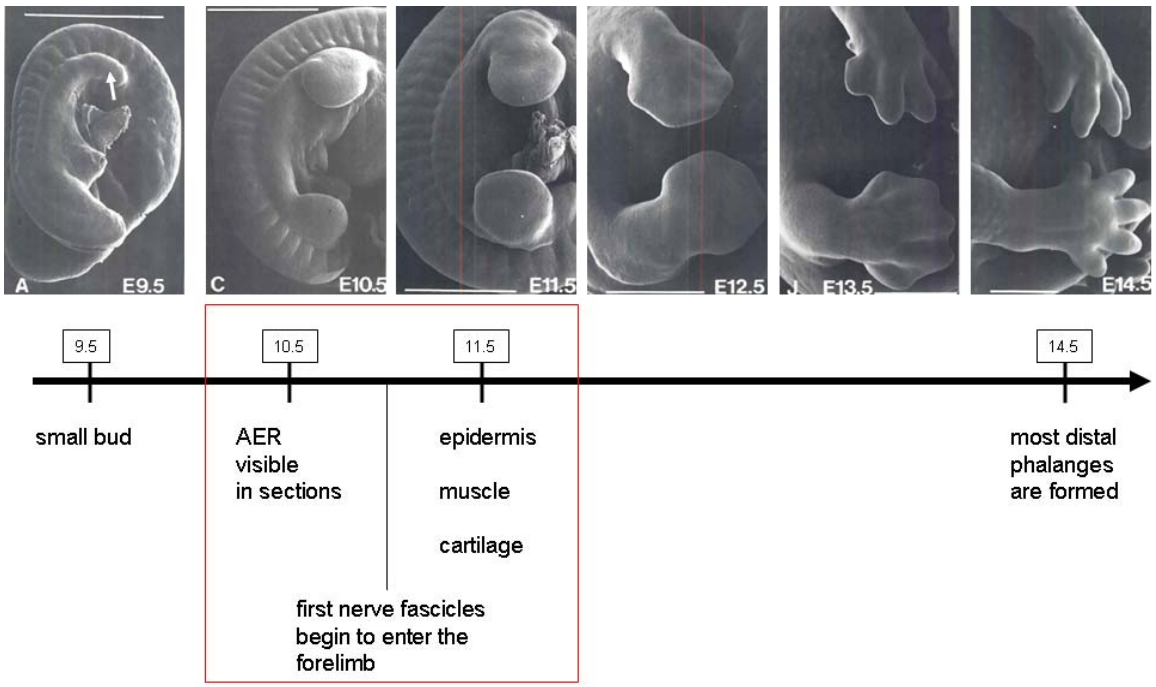

Fig.1.1 - Forelimb development of the mouse. The apical ectodermal ridge (AER) begins to form at E10.5. A two layered epidermis, the first myogenic cells and the first cartilaginous elements can be detected at E11.5. Between E10.5 and E11.5 the first nerve fascicles begin to enter the forelimb. Modified from (Martin 1990).

1.2.2 Innervation of the forelimb

The forelimb is innervated by the brachial plexus, formed from spinal nerves of the fourth cervical to the first thoracic segment, with a small contribution of the nerve of the second thoracic segment (Martin 1990). They form three trunks that separate and refasciculate to establish finally the nerves innervating the forelimb (Fig. 1.2).

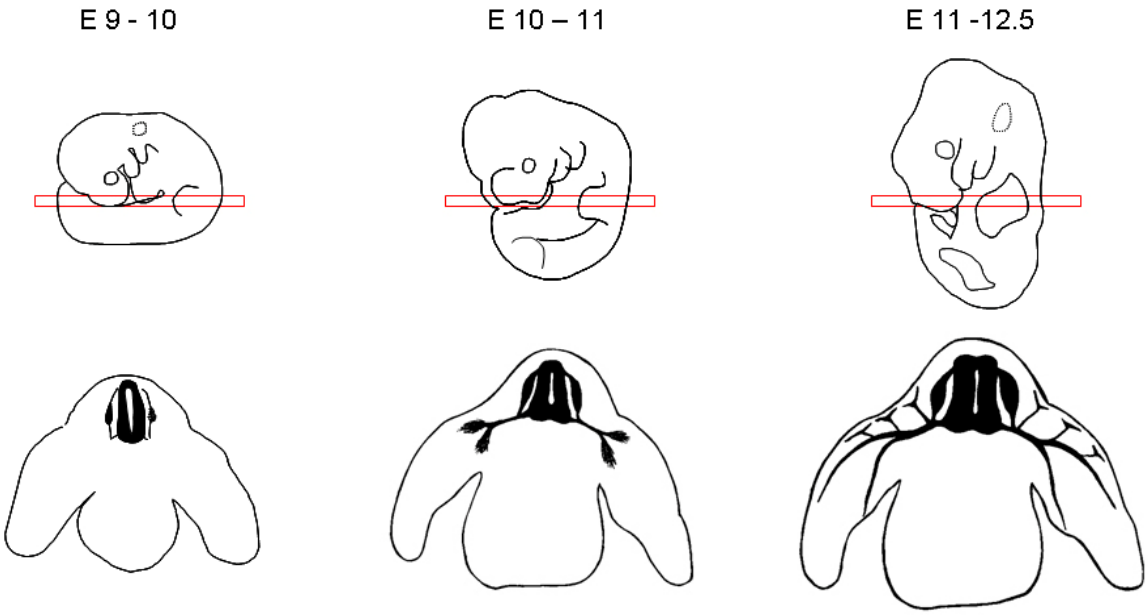

Fig. 1.2 - Forelimb and spinal nerve development from embryonic day (E) E9 to E12.5 in the mouse. **At E9-10** newborn motor neurons situtated in the mantle zone of the ventral neural tube initiate axons that project ventrolaterally. Sensory neurons born in the dorsal root ganglia (DRG) elaborate bifurcated processes, one in the direction of the dorsal neural tube, the other end ventrally to reach the axons of the motor neurons and form the spinal nerves. **At E10-11** the ventral and dorsal roots have formed the spinal nerves, that re- and defasciculate to form the brachial plexus with the trunks, that separate into the dorsal and ventral cords. **At E11.5** the dorsal and ventral cords proceed to extend along the length of the limb and laterally projecting rami develop.

1.3 Guidance cues and receptors

1.3.1 Molecular mechanisms of guidance

Establishing a properly connected nervous system during embryonic development depends on the correct pathways that need to be taken by migrating neuronal precursors, axons, and dendrites. For the regulation of these pathways sets of guidance cues are expressed in part very dynamically and specifically during development.

Axons and dendrites have a highly motile and very sensitive structure, called the growth cone, that allows them to find their way in the developing embryo (Dickson 2002). Such a growth cone is either attracted or repelled by extracellular guidance cues that operate either at close range or over a distance (Tessier-Lavigne and Goodman 1996). These molecular guidance cues can be grouped into several categories (Table 1): adhesive cues, trophic signals, tropic guidance cues, and modulatory guidance cues (Raper and Mason 2010). In addition, growth cone steering also depends upon the presence of intracellular molecular components essential for signaling events (Tran et al., 2007).

categories of guidance cues	members	functions
adhesive cues	extracellular components and cell adhesion molecules	promote extension
trophic signals	neurotrophins, insulin-like growth factor, hepatocyte growth factor	promote neuronal survival, growth cone motility and axon outgrowth
tropic guidance cues	semaphorin3A, netrin, DSCAMs, ephrins	impart a directional valence to growth cone motility, acting as attractants or repellents
modulatory guidance cues	laminin, NGF, chemokine SDF1	affect how axons respond to tropic cues

Table 1 - Categories of guidance cues according to (Raper and Mason 2010).

1.3.2 Semaphorins

Semaphorins are a large family of secreted and membrane-associated proteins, comprising 20 members in mice and humans (Yazdani and Terman 2006). The first described members were fasciclin IV (Kolodkin et al., 1992) and collapsin (Luo et al., 1993) which were later renamed into Sema1a and Sema3A, respectively (Semaphorin Nomenclature Committee 1999). According to their overall structural and phylogenetic characteristics, the family is categorized into eight subclasses, class 1-7 and V (Fig. 1.3) (Semaphorin Nomenclature Committee 1999). Semaphorins of class 1 and 2, and one member of class 5 (5c) are specific for invertebrates, classes 3-7 are present in vertebrates and class V is viral (Khare et al., 2000; Yazdani and Terman 2006; Zhou et al., 2008). Common to all members is the semaphorin domain, a ~500-amino acid extracellular domain (Kolodkin et al., 1993; Puschel 1996; Semaphorin Nomenclature Committee 1999). Although initially described for their role as guidance molecules in nervous system development, they also have diverse functions in the immune system (Yamamoto et al., 2008), the vascular system (Kruger et al., 2005), during organogenesis of the heart (Brown et al., 2001; Feiner et al., 2001), the lung and the kidney (Kagoshima and Ito 2001; Villegas and Tufro 2002), and in the formation of bone and tooth (Behar et al., 1996; Loes et al., 2003). There is furthermore evidence that semaphorins are involved in several diseases, such as schizophrenia, cancer (Kruger et al., 2005), epilepsy (Yaron and Zheng 2007) and neurodegeneration (Roth et al., 2009).

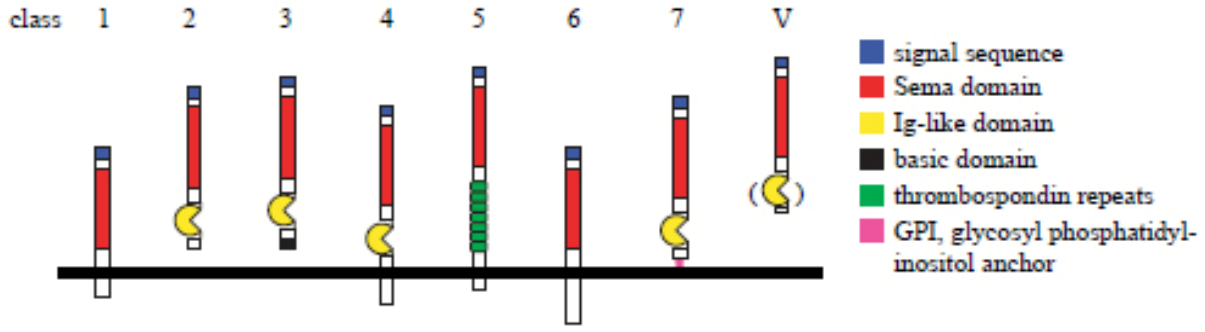

Fig. 1.3 - The semaphorin family (Pasterkamp and Verhaagen 2006).

1.3.3 Semaphorin3A

One of the most intensely studied semaphorins is the semaphorin3A (Sema3A). Initially described as collapsin1, it was the first characterized chemorepulsive protein in vertebrates (Luo et al., 1993). As a member of subclass 3, it is a secreted protein, which is synthesized as a proprotein and requires to be proteolytically processed in order to become repulsive for neurites (Adams et al., 1997). An important binding partner for Sema3A in the extracellular space is chondroitin sulfate (CS). Studies on cortical interneurons revealed the influences both molecules have on each other, and the same dependence might occur in the posterior sclerotome (Zimmer et al., 2010).

In accordance with its very dynamic expression pattern during embryonic development (Messersmith et al., 1995; Puschel et al., 1995; Wright et al., 1995; Puschel et al., 1996; Kawasaki et al., 2002; Anderson et al., 2003), Sema3A is involved in a huge variety of developmental processes. During establishment of the nervous system it was shown to guide sensory and motor neurons (Shepherd et al., 1997; Varela-Echavarria et al., 1997; Huber et al., 2005), to presort striatal neurons (Marin et al., 2001) and axons in the olfactory system (Imai et al., 2009; Miyamichi and Luo 2009), and importantly to repel migrating progenitor cells (Bagnard et al., 2001). In addition to its function as a guidance cue and mediator of timing and fasciculation of motor and sensory axon outgrowth, it can also induce apoptosis (Bagnard 2001). Besides its functions on neurons, it controls cell migration of thymocytes and NC cells (Gammill et al., 2006; Lepelletier et al., 2007; Schwarz et al., 2009; Schwarz et al., 2009; Kulesa and Gammill 2010), repels endothelial cells (Guttmann-Raviv et al., 2007), and is important for heart, bone, lung and vascular development (Behar et al., 1996; Ito et al., 2000; Gu et al., 2003; Schwarz et al., 2004). Furthermore, it was shown to be accumulated in the hippocampus during Alzheimer's disease (Hirsch et al., 1999), involved in multiple sclerosis (Williams et al., 2007), ischemia (Hou et al., 2008), and increased in the cerebellum in schizophrenia (Eastwood et al., 2003).

1.3.3.1 The receptor complex for Semaphorin3A

Semaphorin3A signaling in the nervous system requires the formation of a receptor complex consisting of at least neuropilin-1 (Nrp-1) and a plexinA (Rohm et al., 2000). Sema3A binds Nrp-1 (He and Tessier-Lavigne 1997; Kolodkin et al., 1997), but since Nrp-1 does not have a signaling ability, a member of the plexinA family is necessary to serve as the signal transducer (Nakamura et al., 2000; Yaron and Zheng 2007). In accordance with this, explanted sensory neurons of Nrp-1 mutant mice do not respond to Sema3A (Kitsukawa et al., 1997). Interestingly, plexins contain a divergent Sema domain at their N-terminus which, in the absence of ligands, silences plexinA1 signaling through intramolecular interactions (Huber et al., 2003). Upon binding of Sema3A to the plexin/neuropilin complex, this autoinhibition is released (Takahashi and Strittmatter 2001). There are at least two more proteins that constitute additional Sema3A receptor components. One of them is the transmembrane glyocoprotein L1 (Schachner 1991), a cell-adhesion molecule of the Ig super family (IgCAM) (Castellani et al., 2000; Castellani 2002; Castellani et al., 2002). It mediates the response of neurotrophic tyrosine receptor kinases (TrkA) and neuronal growth factor (NGF) dependent axons to Sema3A in the dorsal horn (Law et al., 2008). The second protein is the receptor tyrosine kinase Off-track (Otk) (Winberg et al., 2001; Toyofuku et al., 2005).

1.3.3.2 Signaling mechanism

Although the repulsive effect of Sema3A has been described for several years, the exact intracellular processes responsible for relaying and integrating the incoming information remain still unclear. Prominent players in the signaling cascade include the Rho family of small GTPases (Halloran and Wolman 2006).

1.4 Function of semaphorin3A on spinal nerves

During vertebrate embryonic development, *Sema3A* is expressed in the developing somites and in the developing limb bud (Tran et al., 2007; Schwarz et al., 2009).

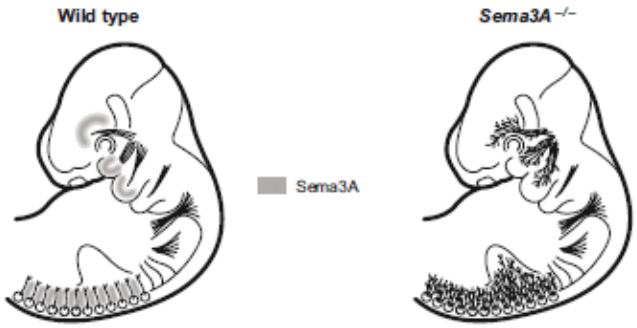

Fig 1.4 - Expression of Sema3A (grey) provides boundaries for the pathfinding of cranial and spinal nerves (modified from Tran et al., 2007)

This expression pattern is dynamic and correlates with a critical period in the pathfinding of sensory and motor neurons (Fig. 1.5).

Fig 1.5 - Dynamic expression pattern of Sema3A mRNA in transverse sections of rat embryos during the development of spinal nerves at the forelimb level (Wright et al., 1995).

It was not only demonstrated to be expressed at the right place to provide a signal necessary for the guidance of spinal neurons, but also to repel DRG neurons cultivated in the vicinity of Sema3A expressing HEK cells (Puschel et al., 1995). Studies on motor neurons of Nrp1 or Sema3A mutant mice revealed that Sema3A controls the fasciculation of lateral motor column motor axons and the timing of motor axon in-growth to the limb, and also provides a dorso-ventral guidance signal in the forelimb (Huber et al., 2005). Surprisingly, Sema3A is also synthesized by motor neurons during axon pathfinding in the chick, setting the sensitivity of their growth cones to environmental sources by locally controlling the availability of Nrp1 at the

growth cone (Moret et al., 2007). Sema3A is not only expressed by mesenchymal cells, but also by the ventral spinal cord. This expression was shown to pattern sensory projections of NGF-responsive axons to terminate in the dorsal spinal cord (Messersmith et al., 1995).

1.5 Function of semaphorin3A in trunk neural crest cells

The role Sema3A plays in trunk NC guidance has only been established during the last two years. Although it was shown to have an effect on cultured chick NC cells (Eickholt et al., 1999) and to be involved in positioning sympathetic neurons (Kawasaki et al., 2002), the more important protein of the secreted semaphorins seemed to be Sema3F.

The firstborn NC cells migrating ventrally alongside intersomitic blood vessels and forming sympathetic neuronal progenitors near the dorsal aorta (Schwarz et al., 2009) are assumed to be positioned near the dorsal aorta due to Sema3A expressed by the notochord and by mesenchymal cells of the proximodorsal forelimb (Kawasaki et al., 2002). The nextborn NC cells are repelled to enter the intersomitic furrow by Sema3A/Nrp1 signaling and migrate through the anterior sclerotome. Their migration into the sclerotome is due to attractive signaling by the stromal cell derived factor-1 (SDF1/CXCL12) (Belmadani et al., 2005; Kasemeier-Kulesa et al., 2010) and confined to the anterior sclerotome by Nrp2/Sema3F repulsion (Gammill et al., 2006), with Eph/ephrin signaling (Wang and Anderson 1997; Davy and Soriano 2007), F-spondin (Debby-Brafman et al., 1999), proteoglycans (Oakley and Tosney 1991), cadherins (Ranscht and Bronner-Fraser 1991), and peanut agglutinin binding gylcoproteins reinforcing this patterned migration (Gammill and Roffers-Agarwal 2010). Expression of Sema3A by the dermomyotome and the ventral spinal cord leads to their positioning lateral to the neural tube and the formation of compact DRGs (Kulesa and Gammill 2010).

1.6 Published semaphorin3A mutant mouse lines

Two Sema3A deficient mouse lines were generated, differing in their phenotype severity, which might be due to different genetic backgrounds. In the mouse line published by Behar et al., most of the homozygous mutants are perinatal lethal, while the homozygous mutants of the line created by Taniguchi et al. are viable into adulthood (Behar et al., 1996; Taniguchi et al., 1997).

Analysis of homozygous mutants revealed projections of sensory neurons into inappropriate regions of the spinal cord, a paucity of neuropil and abnormally oriented neuronal processes in the pyramidal neurons, abnormal development of certain embryonic bones and cartilaginous structures, a postnatal severe hypertrophy of the right ventricle of the heart, and a dilation of the right atrium (Behar et al., 1996). Taniguchi et al. described severe abnormalities in the following peripheral nerve projections: the trigeminal, facial, glossopharyngeal, vagus, and accessory, nerves, but not in the oculomotor nerve. Additionally, they described axons leaving the DRGs from their lateral side instead of leaving ventrally and a disrupted shape of the sympathetic chains. A further analysis performed by White and Behar on spinal nerves also showed aberrant projections from the DRG together with multiple defasciculations in the regions of the dorsal and ventral rami (White and Behar 2000).

All these analyses had been performed only on fixed tissue at definite time intervals during embryonic development. The purpose of the present investigation was to establish an in vitro model for developmental studies and to address the following questions:

1. Do mouse spinal nerves reveal “waiting period” events as it was described for chick (Tosney and Landmesser 1985; Wang and Scott 2000)?
2. Can outgrowth rates and velocities for distinct nerves and their branches be compared?
3. Do motor and sensory neurons respond to short or medium range cues as it is described for cell culture systems?
4. Do spinal nerves of Sema3A homozyogous mutant embryos show key features that are found in mutant embryos of the corresponding embryonic age (Behar et al., 1996; Taniguchi et al., 1997)?

2 Materials and methods

2.1 Materials

2.1.1 Equipment

Autoclave Fedegari FVA3	INTEGRA Biosciences GmbH, Fernwald, Germany
Biostation IM	Nikon, Japan
Centrifuge MIKRO 20	Hettich, Tuttlingen
Confocal microscope C1si with spectral analysis	Nikon GmbH
CO_2 incubator, HERA cell 150	Kendro laboratory products GmbH, Thermo scientific
Cryostat CM3050 S	Leica Microsystems, Nussloch
Digital CCD camera F-View II	Soft Imaging Systems GmbH, Münster
Digital camera COOLPIX 5000	Nikon, Japan
Electrophoreses chamber	Feinmechanikwerkstatt der Universität Heidelberg
Curix60 table top processor	Agfa
FACSCalibur	BD Biosciences, San Jose, CA
Fluorescence microscope BX61WI	Olympus Germany GmbH, Hamburg
Fluorescent confocal laser scanning microscope C1Si	Nikon Instrument Europe B.v.
Gel documentation system *Imagedoc*	Herolab GmbH Laborgeräte, Wiesloch
Hybridisation Incubator 7601	GFL Gesellschaft für Labortechnik mbH, Germany
Incucell incubator	MS Laborgerätehandel, Wiesloch
Inverse fluorescent microscope CKX41	Olympus Germany GmbH, Hamburg
Oven Heraeus	Kendro, Thermo scientific
PCR cycler T*personal*	Whatmann Biometra, Goettingen
Seven easy pH meter	Mettler, Toledo

Spectrophotometer Ultrospec 3100 pro	Amersham, Biosciences
SIGMA laboratory centrifuge 2-5	SIGMA Laborzentrifugen GmbH, Osterode, Germany
Stereozoom microscope Nikon SMZ800	Nikon, Japan
Sterile hood, LaminAir model 1.2	Holten, Denmark
Vibratome for fixed tissue	Leica Microsystems, Nussloch
Vibratom HM 650 V for unfixed tissue	Microm International GmbH
Video Copy Processor P91W	Mitsubishi Digital Electronics America, Inc., Irvine, CA, USA
Ultra Pure Water Purification System	membraPure GmbH, Germany
Water bath	Memmert, Schwabach

Equipment of the BX61WI

Objectives

4x / 0.10	∞/-	PL series	Olympus
10x/ 0.30	∞/-	UPLFL-PH series	Olympus
20x/0.50	∞/-	UPLFL-PH series	Olympus
20x/0.4	∞/0	LMPLFL series	Olympus
50x/0.9 Oil Iris	∞/-	PL series	Olympus
100x/1.25 Oil	∞/-	PLC series	Olympus

Filter

U-MNU2	Olympus
U-MNIBA2	Olympus
U-MNG2	Olympus

Special Software

AnalySIS	Soft Imaging Systems GmbH, Münster
Adobe Photoshop 7.0 and CS4	Adobe Systems
EndNote X3	Thomson Reuters

EZ-C1 Free Viewer 3.30	Nikon
ImageJ	Wayne Rasband NIH
NIS viewer 3.0	Nikon Instrument Europe B.v.
4D Client	4D

Dissection tools

Tungsten, AU plated 3-5%	California Fine Wire Company
Fine forceps	Fine Science Tools, Germany
Scissors	Fine Science Tools, Germany
Insect pins	Emil Arlt Elephant needles
Shortened fire polished Pasteur pipettes	WU Mainz

2.1.2 Consumables

Cellstar culture dishes and plates	Greiner Bio-One GmbH
Conical test tubes, RNase free, 15ml / 50 ml	np nerbe plus
Cover glass 18 mm, No 1.5	VWR International
Coverslips Assistent13 mm / 18 mm	Glaswarenfakrik Karl Hecht, Germany
Hybond-N+ membrane	Amersham Biosciences
Loctite 406	Henkel, Germany
Menzel-Gläser superfrost ultra plus	Thermo Scientific
Microscope slides	Roth, Karlsruhe
Micro tubes (1.5 ml / 2 ml)	Sarstedt, Germany
Millicell-CM insert (PICMORG50)	Millipore corporation
PCR cup (G002 / G003)	G. Kisker GbR
Safe-Lock tubes 1.5 ml / 2.0 ml	Eppendorf
Stericup Filter Unit 0.22 µm	Millipore corporation
Sterile pipettes	Gibco, Invitrogen
Syringe driven filter unit 0.22 µm/ 0.45 µm	Millipore corporation
Tissue freezing medium	Jung, Leica, Nussloch, Germany

Tissue freezing molds	Polysciences Europe, Eppelheim, Germany
Razor blades	Thermo Fisher
3 MM Chromatography paper	Whatman Int., England

2.1.3 Reagents

Agar	Merck, KGaA, Darmstadt
Agarose, NEEO Ultra - Qualität	Roth, Karlsruhe
Benzyl benzoate, minimum 99.0%	Sigma-Aldrich
Benzyl alcohol 99+%	Sigma-Aldrich
DMSO	Acros Organics
Ethanol absolut puriss	Sigma-Aldrich
Ethidium bromide	Fluka
Glacial acetic acid	Sigma-Aldrich
Isopropanol	AppliChem
Nitric acid	Mallinckrodt Baker B.V.
Orange G	Sigma-Aldrich
Roti-Phenol	Roth, Karlsruhe

2.1.3.1 Reagents for cell culture

BDNF	Prof.Yves-Alain Barde
DMEM (41966)	Gibco, Invitrogen
Chick embryonic extract	extracted in the lab
Collagen	extracted from rat tails
Dispase	Gibco, Invitrogen
HBSS 10X (14180)	Gibco, Invitrogen
HEPES f.d. Gewebezucht	Roth, Karlsruhe
FBS and FCS	Gibco, Invitrogen
Fibronectin	Sigma-Aldrich
Laminin	Sigma-Aldrich
L-Glutamine 200mM (25030)	Gibco, Invitrogen

Neurotrophin	Prof. Yves-Alain Barde
NGF	Prof. Yves-Alain Barde
OPTI-MEM reduced serum mix 1X (11058)	Gibco, Invitrogen
Pen Strep (14140)	Gibco, Invitrogen
PLL	Sigma-Aldrich
Propidium Iodide	Sigma-Aldrich
Human recombinant Semaphorin3A / Fc Chimera	R&D Systems GmbH
Trypsin 2,5 %	Gibco, Invitrogen

2.1.3.2 Enzymes and molecular weight markers

taq-polymerase	stock prepared by Xiao Shen, AG Tucker
Proteinase K	Roth, Karlsruhe
100 bp ladder	Fermentas
1kb bp ladder	Invitrogen
λHind	Fermentas
2-Log DNA ladder (0.1 – 10.0 kb)	New England BioLabs

2.1.3.3 Restriction enzymes

BamH I	BioLabs and Fermentas
NotI	Fermentas
SalI	Fermentas

2.1.3.4 Kits

GenElute HP Plasmid Midiprep Kit	Sigma-Aldrich
Nucleospin Extract II	Macherey und Nagel
QIAEX II Agarose Gel Extraction Protocol	Qiagen, Hilden
ProbeQuantTM G-50 Micro Columns	Amersham, Biosciences

2.1.3.5 Plasmids

pEGFP-N1	AG Tucker, Heidelberg
pBK-AP-Flag-Sema3AP1b (717)	AG Püschel, Münster

2.1.3.6 Primer/Oligonucleotides

Oligonucleotides

The following oligonucleotides were ordered from Thermo Fisher Scientific GmbH and used for genotyping.

WT-F	5'-CTC AGC ATC CCA CCT GTA AC-3'
WT-R	5'-CCA GTT GTG TAT GTC CAC CC-3'
EGFP-F	5'-CAG GCT TTG AAC CAG TAT GG-3'
EGFP-R	5'-TGA ACT TGT GGC CGT TTA CG-3'
Sema-R	5'-AGC GCG TCT AGT GAG TGT TG-3'
Sema-N	5'-CGA GGA AGC AGA ATG AAA GG-3'
NeoN	5'-CTT CCA TTT GTC ACG TCC TG-3'

dNTPs	Fermentas

2.1.3.7 Immunohistochemistry

Aqua-Poly/Mount	Polysciences Europe, Eppelheim, Germany
Roti-Liquid Barrier Marker	Roth, Karlsruhe
Triton X-100	Roth, Karlsruhe

Sera, Dyes, and Antibodies

Bovine serum albumin	Roth, Karlsruhe
Newborn calf serum	Gibco, Invitrogen
Native goat serum	Gibco, Invitrogen
Horse serum	Gibco, Invitrogen

Dyes

Alcian Blue 8 GX	Sigma-Aldrich
DAPI	Molecular Probes, Invitrogen
DiI (D3911)	Molecular Probes, Invitrogen
Phalloidin	Sigma

2.1.3.8 Primary antibodies

Epitope	Species		Dilution	Source
Brn3a/ 3.0	rabbit	polyclonal	1:1000	Eric Turner, USA
Cleaved caspase-3 Asp175	rabbit	monoclonal	1:200	Cell signaling
GFP	rabbit	polyclonal	1:1000	Abcam
EGFP	rabbit	polyclonal	1:1000	Uli Müller
Ki-67	rat	monoclonal	1:50	DakoCytomation, Denmark A/S
MyoD	mouse	monoclonal	1:1000	BD Pharmingen
p75	rabbit	monoclonal	1:500	Chemicon
TuJ1	mouse	monoclonal	1:1000	Chemicon
TH	sheep	polyclonal	1:500	Millipore
2H3	mouse	monoclonal	1:20/1:100	Developmental Studie Hybridome Bank, Iowa, USA

Table 2.1 - Primary antibodies.

2.1.3.9 Secondary antibodies

Name	Dilution	Source
goat anti-mouse AlexaFluor 488	1:1000	Invitrogen
goat anti-mouse AlexaFluor 546	1:1000	Invitrogen
goat anti-rabbit AlexaFluor 488	1:1000	Invitrogen
goat anti-rabbit AlexaFluor 546	1:1000	Invitrogen
Donkey anti-sheep AlexaFluor 546	1:1000	Invitrogen
Donkey anti-rat Alexa Fluor 546	1:500	Invitrogen
HRP conjugated goat anti mouse	1:200	Dianova GmbH

Table 2.2 - Secondary antibodies.

2.1.4 Animals

2.1.4.1 Mice

Mouse embryos (*Mus musculus domesticus*) of four different mouse lines were used for cell and tissue culture experiments.

mouse line	method used for	source
tauGFP	slice culture	AG Tucker, IBF Heidelberg
tauSEM	slice culture, cryosections, vibratome sections	AG Tucker, IBF Heidelberg
M22	slice culture, cryosections,	lab of Yves-Alain Barde, Basel AG Tucker, IBF Heidelberg
CD-1	DRG cultures, neural crest cultures	Charles River

Table 2.3 - Mouse lines

2.1.4.2 Rats

Tails of rats (*Rattus norvegicus*), that were used for other experiments, were achieved to extract collagen for tissue culture experiments.

2.1.4.3 Chicken

Chicken (*Gallus gallus*) eggs of the strain white leghorn from LSL RHEIN-MAIN, Dieburg, Germany, were used for preparing chick embryonic extract.

2.1.5 Solutions and buffers

1x PBS (pH 7.4)	140 mM NaCl
	2.7 mM KCl
	10 mM Na_2HPO_4
	1.8 mM KH_2PO_4

2.1.5.1 Gel electrophoresis

50x TAE	1M TRIS
	0.5 M EDTA pH 8
	Glacial acetic acid 57.1 ml
TBE 0.5x	0.045M Tris-borate
	0.001M EDTA
10x OrangeG	50 % Glycerol
	50 % 1X TAE
	0.6% OrangeG
Ethidium bromide	0.5 µg/ml in 1x TAE
Lysis buffer (tail buffer)	100 mM Tris-Cl (pH 8.5)
	5 mM EDTA (pH 8.0)
	0.2% (w/v) SDS
	200 mM NaCl
	100 µg/ml Proteinase K

TE (pH 8.0)	10 mM TRIS/HCl (pH 8.0)
	1 mM EDTA (pH 8.0)

2.1.5.2 Solutions for microbiology

LB-Medium	1% (w/v) NaCl
	1% (w/v) Trypton
	0.5% (w/v) yeast extract
Agar plates	1.2% bacto-agar
	0.8% (w/v) bacto-tryptone
	0.8% (w/v) bacto yeast extract
	0.8 % NaCl
Ampicillin	50 mg/ml

2.1.5.3 Solutions for Southern Blot

Denaturizing Solution	1.5 M NaCl
	0.5 N NaOH
Neutralizing Solution	1 M Tris (pH 7.4)
	1.5 M NaCl
20 x SSC	3 M NaCl
	0.3 M Na-citrate, pH 7.0
Church buffer	0.17 5 (v/v) Na_2HPO_4
	1% (w/v) Bovine Serum Albumin
	1mM EDTA
	7% (w/v) SDS
	35.5 g/l NaH_2PO_4

2.1.5.4 Solutions for immunohistochemistry

Antigen retrieval buffer (pH 6,0)	10 mM Tri-Sodium-Citrate (dihydrate)
Blocking buffer	1% BSA 5% NGS 0.1% - 0.5% TritonX-100 1x PBS
Washing solutions	30% Methanol 1x PBS / 0.1% Triton X-100 50% Methanol 1x PBS / 0.1% Triton X-100 70% Methanol 1x PBS / 0.1% Triton X-100

2.1.5.5 Fixatives

4 % PFA (pH 7.3)	4% PFA 2 N NaOH 1x PBS
8% PFA / 8 % Sucrose (pH 7.3)	8% PFA 8% Sucrose 2 N NaOH 1x PBS
Bouin's solution	75% saturated aqueous picric acid solution 25% Formaldehyde (40%) 5% glacial acetic acid

2.1.6 Culture medium and buffers

2.1.6.1 Solutions for slice culture

HEPES buffer (pH 7.3)	10 mM HEPES
Dissection buffer	1x Ca^{2+}-Mg^{2+}-free HBSS 10 mM HEPES buffer 500 U/ml Pen Strep
Slice culture medium (pH 7.3)	DMEM 25 % 1x HBSS 25 % FBS 0.5 % glucose 1 mM L-glutamine 2.5 mM HEPES

2.1.6.2 Solutions for cell culture

MEF medium	DMEM 10 % FBS 100 U/ml penicillin/streptomycin 2 mM L-Glutamine
CRYO/freezing medium	20 % DMSO (tissue culture grade) 30 % FBS 50 % DMEM
DRG culture medium	MEF 10 ng/ ml NT3 10 ng/ ml NGF 10 ng/ ml BDNF

Neural crest culture medium	MEF
	Chick embryonic extract

2.1.7 Bacteria and eukaryotic cell lines

2.1.7.1 Bacteria

Escherichia coli DH5α	AG Tucker, Heidelberg

2.1.7.2 Eukaryotic cell line

HEK293T: Human embryonic kidney tumour cell line	Prof. Unsicker, Heidelberg

2.2 Methods

2.2.1 Animal handling

All mouse experiments were conducted according to the guidelines of the University of Heidelberg and the State of Baden-Württemberg.

2.2.1.1 Transgenic lines

All mice were kept in the animal facility of the University of Heidelberg (IBF) exposed to light from 6 am to 6 pm. Matings were ordered using the 4D Client (Tierbase) and female animals were controlled for vaginal plug each day by the animal care taker. Noon of the day the vaginal plug was observed was designated as embryonic day (E) 0.5.

TauGFP mice

The *tauGFP* mouse line was generated as described in Tucker et al., 2001 and had been backcrossed more than 10 generations to the C57BL/6 background in order to maintain it as a homozygous mutation. It was already at the IBF Heidelberg and only had to be maintained here.

TauSem mice

The *tauSEM* mouse line was generated by crossing mice of the *tauGFP* mouse line to mice carrying a knockout for the Semaphorin3A (*Sema3A*) (Behar et al., 1996), which were received from Prof. Reha Erzurumlu, University of Maryland, USA. Since the Sema3A knockout mouse in the C57BL/6 background is perinatal lethal as a homozygote (Behar et al 1996) mice homozygous for *tauGFP* and heterozygous for *Sema3A* had to be established and were mated to obtain homozygous-deficient *Sema3A* embryos in a Mendelian ratio per litter of E10.5 – 12.5. Animals resulting from these matings are termed *tauSEM* in this study.

M22 mice

The M22 mouse line was imported from the lab of Prof. Yves Alain Barde at the Neurobiology Biozentrum of the University of Basel, Switzerland. After a rederivation at the IBF of the University of Heidelberg, we received three litters to set up the new colony.

Although the insertion sites for the tauEGFP constructs are random, the animals could be genotyped using the KO primer pairs employed also for PCR reactions on *tauGFP* mice. This

allowed to screen the WT animals out and to restrict further matings to heterozygous animals. However, the bands achieved using PCR didn't give us any information about the number of inserts each animal carried. Therefore, 3 rounds of Southern blot analysis (analyzing the DNA of 33 M22 animals) were employed to eventually achieve a colony consisting of animals carrying the maximal number of *tauGFP* constructs.

Offspring from matings between M22 and tauGFP animals are termed M22-tauGFP in this study.

2.2.1.2 CD-1 mice

Due to a limited cage contingent at the IBF and some additional financial limits we ordered pregnant CD-1 mice from Charles River to perform preliminary experiments for the DRG explant cultures and the neural crest cultures.

2.2.2 Microscope setup

To minimize construction costs for a heating chamber that surrounds the microscope, a macrolon box was planned and set up by ourselves. The side panels and the lid were cut in the proper size in a Fachmarkt for Plexiglas. Both the windows to guarantee access to the stage and the microscope, and the openings for the camera and the burner were drilled at place, following measurements at the microscope. In a final step drill holes were apposed and pieces were screwed together.

2.2.3 Molecular biology

2.2.3.1 Isolation of genomic DNA from embryonic tissue and tail samples

This protocol is a modification of Laird et al. 1991 and was used for genotyping colony animals and embryos.

To each tail biopsy or tissue sample of embryos 500 µl of lysis buffer containing 100 µg/ml Proteinase K were added. Digestion was performed over night at 50° - 55°C under agitation. Hair and tissue residues were sedimented in a centrifugation step at 13.000 rpm for 5 min at room temperature and each supernatant was transferred to a fresh 1.5 ml Eppendorf tube before 500 µl ice-cold isopropanol were added. Samples were vortexed thoroughly and centrifuged at 4°C at 13.000 rpm for 15-30 min. Again, each supernatant was discarded and the

pellet washed with 200 µl of 70% ethanol in a centrifugation step at 4°C at 13.000 rpm for 5 min. As much 70% ethanol as possible was removed by aspiration and pellets of DNA were air dried and dissolved in 30-60 µl of TE by incubation under agitation.

2.2.3.2 Polymerase chain reaction

DNA fragments were amplified using taq-Polymerase which was applied in optimized concentrations (achieved by Xiao Shen, protocol available in the AG Tucker). Specific primer pairs were used for the WT and KO reaction to genotype *tauGFP* and tauSEM mice or embryos. For amplification of the Sema3A specific DNA fragments it was critical to use PCR tubes from Kisker (Germany).

A standard PCR mix was as follows:

15.9 µl	H_2O
2 µl	10x PCR reaction buffer
0.8 µl	50 mM $MgCl_2$
0.4 µl	10 µM Primer 1
0.4 µl	10 µM Primer 2
0.4 µl	10 mM dNTPs
0.1 µl	Taq- polymerase
0.2 µl	DNA (10-100 ng)

2.2.3.3 Gel electrophoresis

Gel electrophoresis was performed to identify the correct DNA fragments from PCR and to control digestion reactions of genomic and plasmid DNA.

For the separation of DNA fragments from PCR and digestions 1% - 1.8% agarose gels were used, prepared of 1x TAE.

Samples supplemented with 10x Orange G in the appropriate volume were loaded and appropriate ladders were used to determine the size of the fragments.

Electrophoresis was performed at 110 V for 30-50 min. Afterwards the gels were incubated for 10-20 min in 1xTAE supplemented with 0.5µg/ml Ethidiumbromide to stain the DNA fragments.

2.2.3.4 Phenol chloroform extraction

Phenol chloroform extraction was used for the purification of DNA, that was used later for Southern blot analysis.

Tail biopsies were digested in lysis buffer containing 100 µg/ml Proteinase K overnight. In the centrifugation step the hair and tissue residues were pelleted and supernatant transferred to 1. 5 ml safe-lock tubes (Eppendorf). An equal volume of Phenol/Chloroform to the volume of lysis buffer was added and vortexed thoroughly. Tubes stood for several minutes at room temperature before they were centrifuged for 5 min at 13000 rpm. The upper aqueous phase containing the DNA was transferred to a new safe lock tube where an equal volume of Chloroform was added. Samples were vortexed and centrifuged for 13000 rpm for 5 min. The upper aqueous phase was transferred into new 1.5 ml safe lock tube and treated with Chloroform for one more time. After the centrifugation the upper phase was transferred to a new 1.5 ml safe lock tube and 1/10 of the final volume 3M NaOAc, pH5.3 was added. 2x the volume of the water phase of Ethanol was added, vortexed and left at -80°C for 1 hour or over night. Centrifuged at 4°C at 13000 rpm. The supernatant was discarded and pellets rinsed with 70% Ethanol. DNA was resuspended in 10 - 30 µl Tris-HCl.

2.2.3.5 Southern blot analysis

Probe synthesis

For the digestion of pEGFP-N1 two restriction enzymes were used: NotI and SalI.
The digestion reaction was prepared as follows:

7 µl	plasmid
2 µl	10x buffer
1 µl	NotI
1 µl	SalI
9 µl	H_2O

The reaction was incubated in a water-bath at 37°C for 3 hours and kept afterwards at -20°C. The digestion efficiency was controlled by electrophoresis on 1% agarose gels containing ethidiumbromide.
To recover DNA from an electrophoreses gel, the fragment of interest was cut out of the gel, put in Eppendorf tubes with known weight and extracted according to the QIAEX II Agarose Gel

Extraction Protocol. The DNA was labeled with α^{32}P-dCTP (Hartmann Analytic GmbH) by using ready-to-go DNA labeling beads (Amersham). Unicorporated labeled nucleotides from the DNA-labeling reaction were removed applying ProbeQuant G-50 Micro Columns (Amersham).

Sample preparation

DNA of tail biopsies was isolated by digestion with Proteinase K as described, followed by a phenol chloroform extraction. The concentration of the DNA was measured in a 1:100 dilution with a spectral photometer at 260 nm. The absorbance of the DNA was measured at 260 nm and 280 nm to determine the purity.

10 µg of genomic DNA were digested using BamHI overnight and fragments were separated by electrophoresis on 0.7% agarose gels containing 0.5 µg/ml ethidium bromide in 1 x TAE buffer. The gel was run at 100 V for 2 hours. After electrophoresis was completed, a picture was taken, and the gel placed upside down in denaturing solution for 45 min. Gel was rinsed with deionized water and and kept in neutralizing solution for 45 min (neutralizing solution was changed after 30 min) on rocker.

Blotting was performed over night by the capillary transfer method (Maniatis et al.) using 10 x SSC as transfer buffer onto a HybondN^+ membrane. After marking the positions of the gel slots and the ladder on the membrane, it was put into a UV-irradiator to crosslink the DNA. Prehybridization was performed

Hybridisation and Detection

Hybridisation was performed over night in Church buffer at 65°C. After the hybridization the membrane was washed twice with 1x SSC/1% SDS at 65°C, followed by washing steps in 0.5x SSC/0.5% SDS and 0.3x SSC/0.3% SDS for another 15 min each. The membrane was then exposed to an X-ray film (Kodak) at -80°C in a cassette with scintillation screens.

2.2.4 Methods of microbiology

Agar plates

Bacto-agar, bacto-tryptone, bacto-yeast extract and NaCl were weighed and put in a 1 l bottle. 800 ml of deionized H_2O were added, bottles were shaked and let stand for 10 min until the solutes had dissolved. Autoclaved solutes, let it cool down to 60°C or less, added desired antibiotics and poured into 10 cm-bacterial plates. The agar was allowed to cool down, and plates were stored upside down and light protected at 4°C.

Transformation

Thawed 100 µl aliquot of competent cells on ice. Added 0.1 – 5 µl of plasmids and incubated on ice for 30 min. Bacteria were heat shocked for 1 min at 42° C, followed by keeping them for 1 min on ice. 900 µl LB medium were added and cells were incubated at 37°C on a shaker (160 rpm). Different volumes (50-200 µl) were plated on bacterial agar plates and incubated overnight at 37°C.

Liquid cultures of Escherichia coli

For medium-scale preparations of plasmid DNA 100 ml of LB-medium that contained either Ampicillin or Kanamycin were inoculated with a single colony of transformed bacteria using a yellow pipette tip. The bacterial cultures were incubated overnight at 37°C shaking at 160 rpm.

Isolation of plasmid DNA

Cell lysis and Midiprep according to the protocol provided by Qiagen for the GenElute HP Plasmid Midiprep Kit. Pellet was dissolved in Tris-HCl and concentration measured.

Sequencing

Plasmids were sequenced at GATC Biotech.

2.2.5 FACS Analysis

Directly after the vibratome slicing procedure, the slices were trypsinized (0.25% Trypsin in PBS, 0.5 mM EDTA pH 8.0) for 10 min in a 37°C water-bath. The trypsin was washed out twice with warm PBS, and the tissue was dissociated by pipetting up and down with a Gilson pipette (200 µl). FACS analysis was performed on a FACSCalibur device (Becton Dickinson, Biosciences, San Jose, CA). Just before FACS analysis, PI (250 ng/ml final concentration) was added to allow quantification of dead cells in the red channel. A proper compensation for the GFP-based fluorescent signal was first determined using cells not labeled with PI. The 50,000 events were counted for each condition, with a sort rate of < 1,000 events per second. Nontransgenic embryos were used as a negative control to estimate background (less than 1%).

2.2.6 Scanning electron microscopy

Slices were fixed overnight at 4°C in 2.5% glutaraldehyde/0.1 M PIPES pH 7.4, washed 3 times in 0.15 M PIPES pH 7.4 at 4° C, treated for 1 hr at room temperature with 1% OsO4, washed 3 times with 0.15 M PIPES pH 7.4, and finally dehydrated in an ascending ethanol series. The slices were transferred in a small steel basket to a CPD 030 critical point dryer (BAL-TEC AG) that was one-third filled with 100% ethanol, and the cap was sealed airtight. Once a temperature of 10°C and a pressure of 50 Bar was reached, the chamber was repeatedly emptied of liquid and filled with CO2 (approximately 6–8 times) without uncovering the sample so that all ethanol was removed. The chamber was then completely filled with liquid CO_2 and heated to a temperature of 40°C and a pressure of 80 Bar. The slices were then sputter-coated with a 5-nm carbon layer in a high vacuum coating system (BAL-TEC MED 020). For SEM, a LEO 1530 field emission scanning electron microscope with a Schottky cathode was used (LEO Elektronmikroskopie GmbH, Oberkochen, Germany).

2.2.7 Cultures

2.2.7.1 Cell cultures

2.2.7.1.1 HEK 293T cell cultures

Frozen 293T cells were thawed in a water bath at 37°C. 1 ml of prewarmed MEF medium was added to a single vial and used to transfer cells into a 15 ml tube. Additional 9 ml of medium were added and mixed carefully. In order to remove the DMSO contained in the freezing medium the cell suspension was centrifuged for 5 min at 800 rpm and the supernatant was discarded. The pellet of 293T cells was gently resuspended in 10 ml prewarmed MEF and transferred to a 10 cm cell culture dish.

Maintaining 293T cells

293T cells were split in regular intervals when reaching 80-90% confluency. The medium was removed from the cultures, the cells were washed with 1x PBS once and 1 ml Trypsin was added. Cultures were placed back into the incubator for 1-2 min, before shaking the plates to ensure the detachment of the cells. To stop the trypsinization 10 ml of MEF medium were added, and used to distribute the cells into new 10 cm cell culture dishes in the desired concentrations.

2.2.7.1.2 Neural crest cultures

Preparation of chick embryonic extract

Chick embryonic extract was prepared from E10.5 and E11.5 chick embryos and used as a supplement for the neural crest culture medium.

Eggs were cleaned with 70% Ethanol, opened with a sterile forceps and embryos were placed in a 10 cm tissue culture plate containing a small volume of CMF. All compact structures of the embryo such as feet, claws, eyes and the beak were removed and the rest of the tissue was minced with scissors. The tissue was disrupted with using a 10 ml syringe. For one embryo 5-7 ml of DMEM were added and homogenated with the tissue. The homogenate was poured in a 15 ml Falcon tube which was kept for 30 min on ice. To achieve a cell clump free extract, the homogenate was centrifuged for 10 min at 2000 rpm. Aliquots were prepared of the supernatant and stored frozen at -20°C.

Preparation of rat tail collagen

Tails were collected from directly killed female rats, cleaned with water and stored at -80°C. Having collected at least 2 tails, they were sterilized in 70% ethanol for 15 min and rinsed in sterile, distilled water. For the preparation the tip of the tail was fixed using a medical forceps and the tail was cut distal to proximal using a scalpel. The skin was removed and the tendons collected into 70% ethanol. Tendons were briefly rinsed with sterile water and transferred to a sterile flask containing an autoclaved magnetic stir-bar and approximately 250 ml of 0.1% acetic acid for each 0.5 g of tendon. The collagen was extracted over night at room temperature, and for another day at 4°C. The solution was then centrifuged for 30 min at 4°C and the supernatant used to prepare aliquots that were stored at -20°C.

Coverslip preparation

To be able to perform fluorescent microscopy most cells are plated onto coverslips that were pretreated to allow cell adhesion. Coverslips were placed in acid-resistant racks and weighed down with a segment of a 2 ml glass pipette. They were rinsed in water and cleaned in a bath of nitric acid for a minimum of 36 hours. Afterwards the coverslips were rinsed thoroughly with VE water over several hours and immersed in 100% Ethanol for 30 min. They were dried and exposed to a UV lamp under a laminar flow hood and stored sterile in 10 cm tissue culture dishes.

Culture plate treatment

For imaging neural crest cultures at the Biostation coverslips were mounted on culture dishes using elastosil and covered with Collagen or Fibronectin.

Collagen was diluted 1:6 in 0.1% acidic acid, Fibronectin in a concentration of 5µg/ml. Incubated at room temperature for a minimum of 2 hours. Both Fibronectin and Collagen were removed. Fibronectin pretreated coverslips were washed with DMEM at least 2 times before usage, Collagen coverslips were allowed to dry and then washed with DMEM.

Neural crest cultures

Primary neural crest cultures were prepared from E 9.0 - 9.75 d.p.c. mouse embryos of timed pregnant mice. The embryos were dissected in 1x PBS on ice. Of E9.0 and E9.5 embryos

the neural tube surrounded by the 8 most caudal somites was cut apart from the embryonic tissue. The epidermis and lateral mesoderm were removed by pulling it away with fine forceps. Neural tubes were transferred to pretreated coverslips placed in 12 or 24 well culture plates and incubated over night.

2.2.7.1.3 Dorsal root ganglion cultures

Timed pregnant mice were killed by cervical dislocation, and embryos at E13.5 dissected. The skin covering the neural tube was carefully removed from the dorsal side and dorsal root ganglia (DRGs) picked by forceps. DRGs were collected in 1x PBS on ice, and afterwards transferred onto 5µg/ml Laminin/ 5µg/ml Fibronectin pretreated coverslips.

2.2.7.2 Slice cultures

Preparation of slice cultures

Noon of the day that the vaginal plug was observed was designated as embryonic day (E) 0.5. Timed pregnant mice were killed by cervical dislocation, and embryos at developmental stages E10.25 – 10.75 were removed from the uterus, cleared of the amnion and chorion, and kept in ice-cold PBS (without Ca^{2+} /Mg^{2+}). Embryos were straightened on a bacteriological plate and embedded in 4% LMP agarose in 1x PBS.

The trunk of the embryo was isolated by cutting with a razor blade, covered successively on the second lateral side with agarose, and mounted with superglue on the chuck of the vibratome, such that the caudal aspect of the embryo was sitting upon the chuck, with the dorsal aspect facing the blade. The 350 – 400 µm slices were cut in Ca^{2+} /Mg^{2+}-free Hanks' balanced salt solution (HBSS) at 4°C, using a HM 650 Microtome with a vibrating blade. Each slice was transferred with a Pasteur pipette into 4-5 ml of HBSS in a six-well plate kept on ice. The agarose was then carefully removed around the slices with fine forceps. 4-5 slices were transferred onto a 3-cm Millicell insert that had been rinsed with culture medium. The membranes were placed into 10-cm Petri dishes with 6 ml of culture medium and placed in an incubator at 37°C and 5% CO_2. Half of the culture medium was changed at least once a day.

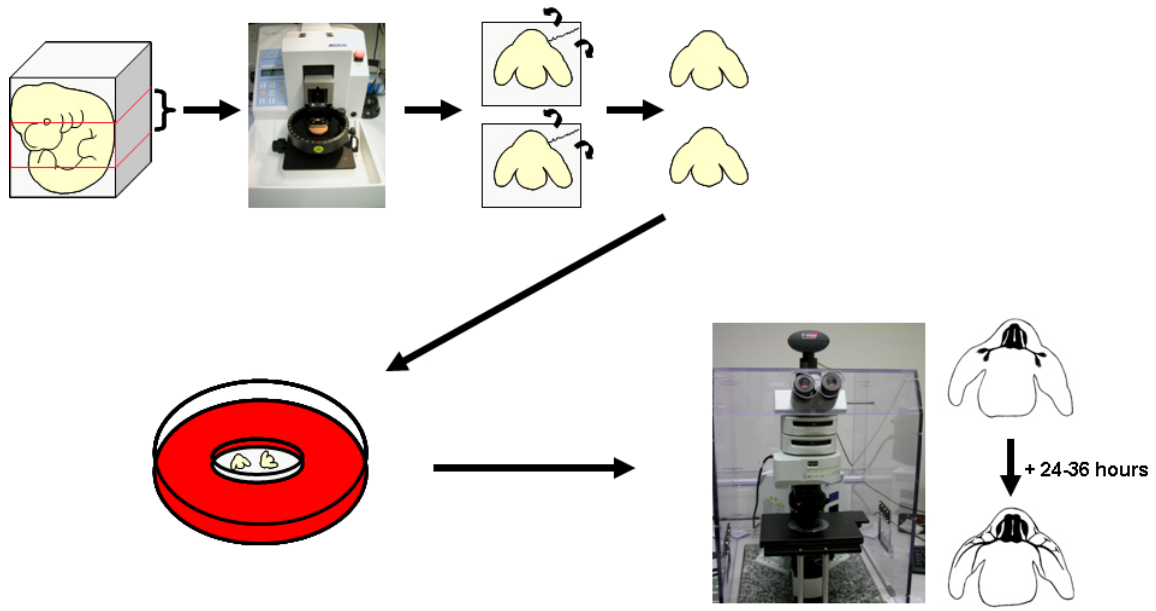

Fig. 2.1 - Preparation of slice cultures. Embryos are embedded in low melting point agarose and cut on a microtome with vibrating blade. The agarose is then removed from the slices and slices are transferred to Millipore culture inserts, sitting in 10 cm culture plates filled with medium. To follow spinal nerve outgrowth, images are taken at regular time intervals under an upright fluorescent microscope.

2.2.8 Immunohistochemistry

Fixation of embryos

Embryos were evicerated, confirmed for EGFP signal under an inverse fluorescent microscope, and placed in 4% PFA for several hours or over night at 4°C, depending on their age. The amnions were collected separately for DNA extraction and genotyping. PFA was washed out with 1 x PBS.

Mounting of embryos

Serial steps of 10%, 20% and 30% sucrose were done before embryos were placed in small "Peel-Away" mounting moulds that had been previously half-way filled with mounting medium (tissue-tek). After 20-30 min, embryos were positioned in the desired orientation. Once the proper orientation was attained, the bottom of the mould was quickly frozen in liquid nitrogen, to fix the embryo in position. To freeze the molds completely, they were placed on dry ice for 20 min and finally stored at -80°C.

Cryosections

Standard conditions for cutting cryosections were: chamber temperature -21°C, object temperature: -19°C. Modifications in temperature and slice thickness had to be introduced to compensate for higher room temperatures during summer time. Sections were collected on microscope slides superfrost, dried and frozen at -80°C.

Vibratome slices of fixed tissue

Fixed embryos were embedded in 4% Agar and cut on a HR2 slicer (MPI für Medizinische Forschung) into 100 µm thick slices. Settings: frequency/Hz: 50.4, amplitude/mm: 1.004, forward / mm/s: 0.15

Immunofluorescent stainings

Cryosections

Slides were removed from minus 80°C and Roti-Liquid Barrier Marker was used to trace an area around the sections on the slide to prevent the liquid spreading all over the slide. The slides were then placed into 1x PBS for rehydration. Excessive 1xPBS was removed and 50-100 µl of blocking solution were added on each slide. After blocking for 1 hour at room temperature, blocking solution was removed and the blocking solution plus the primary antibodies was added. Sections were incubated overnight at 4°C. The next day four washes 4 x 10 minutes in 1xPBS were performed, followed by an incubation with the secondary antibodies. Incubation took place for 2 hours at room temperature or overnight at 4°C. Again, the slices were washed 1x with DAPI in 1x PBS and 3 x 10 min in 1x PBS and dunked in water. After removing as much liquid as possible, slices were mounted with coverslips using aqua polymount.

DRGs and neural crest cells

The same protocol as described for the cryosections was employed. The coverslips were placed on Parafilm lying in a humid chamber for stainings and washing steps. Cells were mounted with slides using aqua polymount.

Vibratome sections

Vibratome sections were stained in 48 well plates. Blocking, incubation and washing steps were performes as described for the cryosections. Slices were mounted with slides and coverslips using aqua polymount.

Antigen retrieval

In order to achieve a staining for the Ki-67 antibody an antigen retrieval was necessary. Cryosections were thawed at room temperature and incubated in 1xPBS. Slides were put in a metal rack which was placed then nto a pressure cooker and covered with buffer. The pressure cooker was heated on a heating plate until it reached full pressure. After cooking sections for 2 min under full pressure, the cooker was removed from the plate and cooled down under running water to remove the pressure. The lid was opened and sections were allowed to cool down staying in the buffer for another 20 min before rinsing them in 1x PBS and water.

Whole mount stainings

Whole mount stainings were performed for Neurofilament M, the neurotrophin receptor p75 and the blood vessel marker pecam (data for the last p75 and pecam are not shown).
Dissected embryos were fixed overnight in 4:1 methanol:DMSO at 4°C. After washing out the fixative with 100% methanol 5 times for 10 min each, the embryos were bleached in 6%H2O2 at 4°C for at least 4 hours and rehydrated by successive steps, 30 min each, in 75%, 50%, 30%, 0% Methanol in PBS/0.1% TritonX-100. Blocking of the embryos was done by incubating for 2 h at RT in 80% FCS:20% DMSO. Embryos were incubated gently rocking with 2H3 anti-neurofilament monoclonal mouse antibody at 4°C for 48 hours. Before and after incubation with the secondary antibody for at least 24 hours at 4°C, embryos were washed at least 10 times in PBS/0.1% TritonX-100 at RT for 6 hours. For the development reaction embryos were first rocked in 0.5 mg/ml DAB in 1x PBS in small glass beakers for 30 min, until 4 µl of 0.3% H2O2 per 5ml of DAB in 1x PBS were added. The reaction was allowed to perform in the dark, however checked at least every 30 min. The coloring reaction was stopped by switching to 1x PBS/0.1%NaN3 washing them several times. For longer storage , embryos were dehydrated by successive steps of 30%, 50%, 70% and 100% methanol in 1x PBS/0.1% TritonX-100, and then cleared in benzyl alcohol: benzyl benzoate 1:2 in glass beakers.

Alcian blue staining

Slices and dissected embryos were fixed in Bouin's solution for 2 hr, rinsed with a solution of 70% ethanol/ 0.1% NH4OH for 12–24 hr in five to eight changes, placed in 5% acetic acid for 2 hr, stained with 0.05% Alcian blue 8GX in 5% acetic acid, rinsed for 2 hr in 5% acetic acid, dehydrated in methanol, and finally cleared in 1:2 benzyl alcohol/benzylbenzoate.

Microscopic analysis and image adjustments

Spinal nerve outgrowth in transverse slices was imaged at a BX61WI upright fluorescent microscope. For measurement of spinal nerve outgrowth the provided software analySIS was used. Neural crest cell cultures were imaged with a Biostation located at the Nikon Imaging Center (NIC) Heidelberg. Images of stained cryosections and vibratome sections were taken at a C1Si-confocal laser scanning system and A1R4 laser line confocal microscope at NIC. Z-stacks were processed using EZ-C1 Free Viewer 3.30 and ImageJ. Whole mount stainings were documented using a Stereozoom microscope connected to a digital (AG Tucker) camera.

3 Results

3.1 A system for imaging neuronal outgrowth

Analysis on axonal outgrowth and pathfinding has been performed extensively and very successfully in cell cultures. However, one would also like to observe and manipulate axonal outgrowth and pathfinding as it occurs within the embryonic tissue itself, in particular to address the function of stiffness, gradients of signaling molecules, and interactions of growth cones and migrating cells with their direct environment.

A great opportunity to analyse neuronal development is offered by transgenic mouselines that express fluorescent proteins specifically in the nervous system. One such engineered mouse line is the *tauGFP* line (Tucker et al., 2001), expressing the enhanced fluorescent protein (EGFP) from the gene *Mapt*, encoding the microtubule-binding protein tau. This locus guarantees EGFP expression specific to postmitotic neurons.

TauGFP mice are viable, fertile, and revealed no significant aberrations during embryonic development of the nervous system (Tucker et al., 2001; Brachmann 2005). The first fluorescent signal is observed at embryonic day (E) 9.0 in the trigeminal ganglion and already 36 hours later it appears throughout the peripheral and central nervous system (Fig. 3.1)

Fig. 3.1 - Expression of EGFP in the developing nervous system of a homozygous E10.5 *tauGFP* embryo. Trigeminal ganglion (V), facial nerve ganglion (VII), vagal nerve ganglion (X), spinal nerves (arrows).

3.1.1 Improvement upon slice culture system

A fast method to prepare transverse slices of several embryos at the same time is to use a guillotine (Tucker 2001). Using this method, a steel grate wrapped serially with tungsten wire is projected with a spring onto embryos lying beneath on a piece of agarose, producing 300-µm-thick sections. Although this method has the advantage of allowing 4-6 embryos to be prepared at one time, it unfortunately damages the tissue and results in only two or three slices per litter that are cut in a proper orientation and that show robust outgrowth of spinal nerves over time. To increase the outcome of properly cut slices, in particular also to make this method suitable to work with mouse mutants, in which only 25% of the embryos in a litter are homozygous mutant for the gene of interest, I introduced a new method of sectioning. The use of a microtome with a vibrating blade offers the advantage to produce sections of any given thickness from individual or several embryos at a time, and furthermore improved the tissue viability drastically.

3.1.2 Establishment of a time lapse imaging system

To perform time-lapse imaging of spinal nerve outgrowth, it is essential to keep the slices directly on the microscope stage, in this case of an upright microscope, since the best outgrowth is achieved when culturing slices on membranes, to guarantee a maximum exchange rate of gas. Hence one major task was to create a stable environment, as to be found in a tissue culture incubator (37°C and 5% CO_2), at the microscope itself. Beginning with a Thermo Plate (TokaiHit MATS-U55), an objective heater, and an 14 cm x 14 cm x 2.5 cm acryl sample box (provided by Olympus, Germany for time-lapse imaging) that was connected to an incubator, none of the imaged slices showed outgrowth for a time period longer than 2 hours. Comparing set-ups that were used for live-imaging by other groups, I decided to improve the system by several components:

1. a macrolon box (constructed by ourselves) that is built around the microscope to keep a reproducible constant environment and to reduce temperature loss through the microscope itself,
2. a heating device with a temperature control (built in the “Elektronikwerkstatt” of the University of Heidelberg), to keep 37°C in the macrolon box, and
3. a system that guarantees a stable CO_2 supply (gas conduit and Leica CTI-controller 3700) modified to use it at an upright microscope instead of an inverse microscope.

3.1.3 Imaging of peripheral nerve outgrowth

The slice cultures have been proven before to be a suitable technique for analyzing peripheral nerve outgrowth in the forelimb region (Tucker et al., 2001). To determine what the limb innervation looks like employing the vibratome slicing method, the first step was to prepare slices of the forelimb and to document their quality and the consecutive nerve outgrowth at specific embryonic stages.

All prepared slices showed an intact tissue morphology, regardless of the developmental stage at which they were prepared (Fig.3.2). The neural tube displayed a strong green signal in the lateroventral half, derived mostly from newborn motor neurons, with commissural connections between the left and right sides. The dorsal root ganglia (DRGs) located adjacent to the upper lateral half of the neural tube showed a strong speckled signal corresponding to individual sensory neurons (Fig.3.2 B and D). Transverse slices of E10.5-E10.75 embryos usually contained one or two intact spinal nerves. At this time, the spinal nerves had entered the forelimb bud and in many slices, the initial division into trunks and subsequently into dorsal and ventral cords had occurred (Fig. 3.2 B). Slices made of E11.0 embryos showed a clear separation of the dorsal and ventral cords (Fig. 3.2 C). In slices of E11.5 embryos, these two nerve cords proceeded to extend along the length of the forelimb (Fig. 3.2 D), and a laterally-projecting ramus from the proximal portion of the spinal nerve could also be observed (Fig. 3.2 D, arrow).

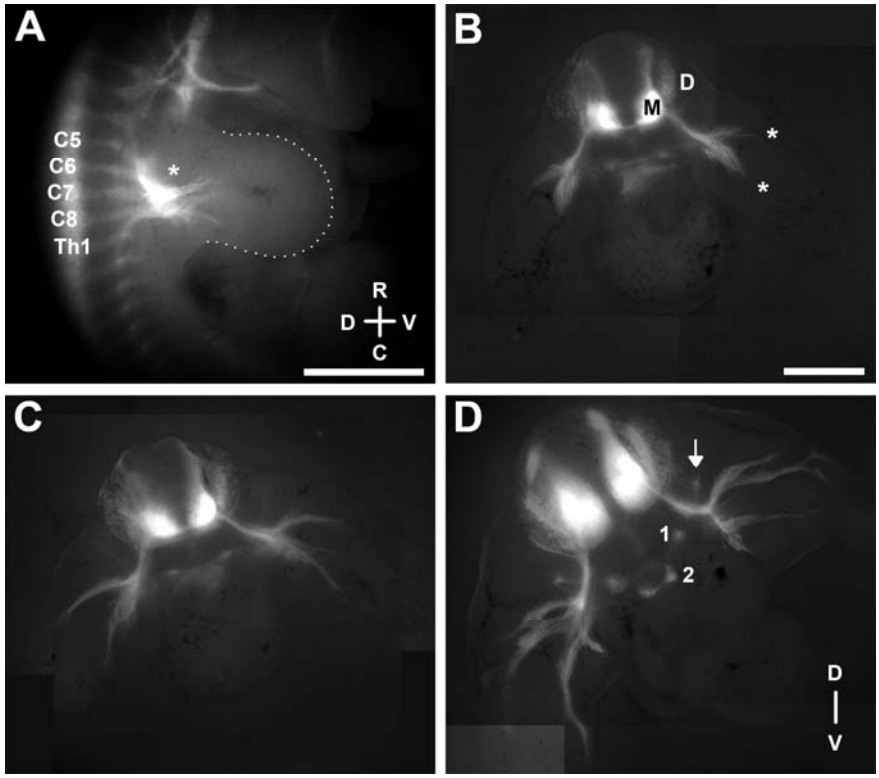

Fig. 3.2 - Forelimb innervation of *tauGFP* embryo. **A**: Sagittal view of the uncut embryo. Brachial plexus (asterisk) of a E10.75 embryo. The DRGs are indicated (C5-Th1) from which the spinal nerves contributing to the forelimb (outline in white dots) are derived. The rostral (R) –caudal (C) and dorsal (D) – ventral (V) axes are indicated. **B-D:** Acute transverse slices from embryos at the axial levels C5-Th1. **B:** At E10.5. The ends of the outgrowing spinal nerves are indicated (asterisks) on the right side of the slice only, as is the DRG (D) and the motor neurons (M) of the ventral spinal cord. **C:** At E11.0. **D:** At E11.5. On the right side of the slice, the nascent suprascapular nerve (arrow), the paravertebral (1) and prevertebral (2) sympathetic ganglia are indicated. The D-V axis is indicated for B-D. Scale bars = 1mm in A, 500 µm in B-D.

In order to reproduce the endogenous developmental pattern of limb innervation *ex vivo,* in a second step we cultured slices from E10.25 to E10.75 embryos and took images at regular time intervals (Fig. 3.3).

At the beginning of the imaging series, sensory projections derived from DRGs have already met motor axons from the spinal cord and formed together the nascent brachial plexus (Fig. 3.3, 5 h). In the three following images (12-18 h) a separation of the trunks into dorsal and ventral cords can be clearly observed, accompanied by a defasciculation at the ends of the cords. The following two images (21-25 h) demonstrate a continued outgrowth of the dorsal and ventral cords and the emergence of a proximal ramus, the nascent suprascapular nerve (Fig. 3.3, 25 h, arrow), that grew toward the lateral edge of the slice. The final two images (33 and 39 h) demonstrate branching of the ventral and dorsal cords into main nerve branches and a more pronounced growth of the ventral cord, while the dorsal cord reached the edge of the forelimb bud.

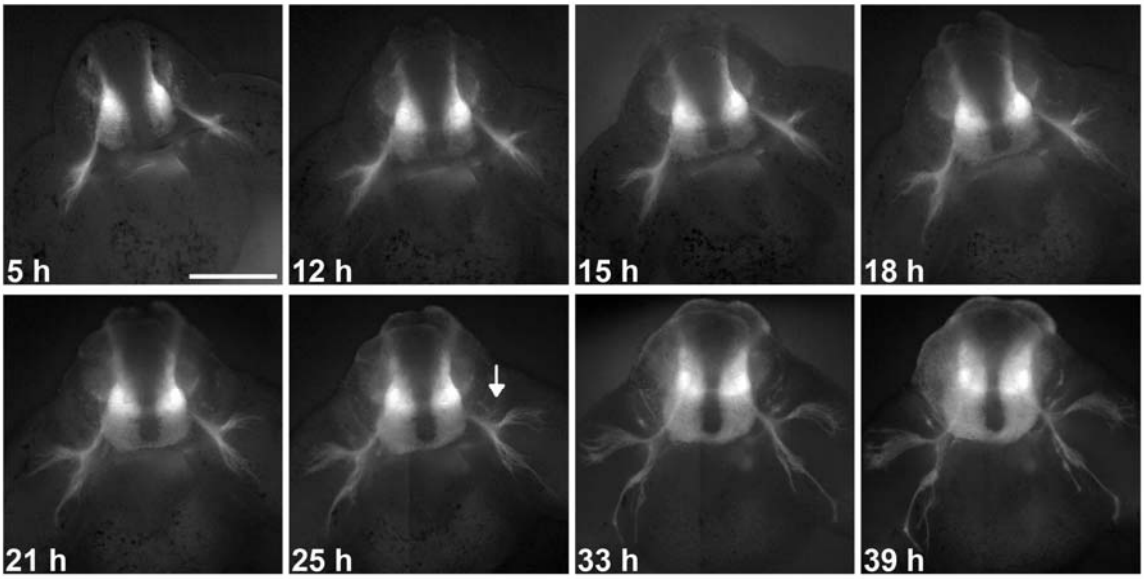

Fig. 3.3 - Timed imaging series of nerve outgrowth in transverse slices of a E10.25 *tauGFP* embryo. The dorsal side of the embryo is at the top of each figure. Hours spent in culture are indicated in the bottom left of each image. Between 21-25 hours the nascent suprascapular nerve (arrow) emerges. Scale bar = 500 µm.

These results reveal a spatiotemporal axonal outgrowth pattern of spinal nerves in the forelimb similar to that *in vivo*, indicating the great suitability of this slice culture system.

3.1.3.1 Measurement of the rate of spinal nerve outgrowth

To observe the outgrowth process at a finer resolution, we focused upon the ends of the outgrowing nerve bundles (Fig. 4.4). Outgrowth was measured in slices prepared from a litter of E10.5 embryos, in which spinal nerves had already formed the nascent brachial plexus and started to branch into dorsal and ventral cords (Fig. 3.4 B). All time series (n > 100) displayed a continuous outgrowth of the dorsal and ventral cords. Motor and sensory axons grew from the neural tube as fasciculated spinal nerves (e.g. derived in (Fig. 3.4 A) from 2 different axial levels), converged into three trunks, defasciculated, and divided into the dorsal and ventral cords (Fig. 3.4, 4 h). At the beginning of the series, the axons of the future dorsal and ventral cords showed a decrease in fasciculation in combination with ongoing outgrowth (Fig. 3.4, 12 h). After the decision to divide into ventral and dorsal cords was made, the more proximal part of the trunks became thinner, and dorsal rami emerged from the proximal portions of the nerves to grow out to the lateral myotome (Fig. 3.4, 22 h).

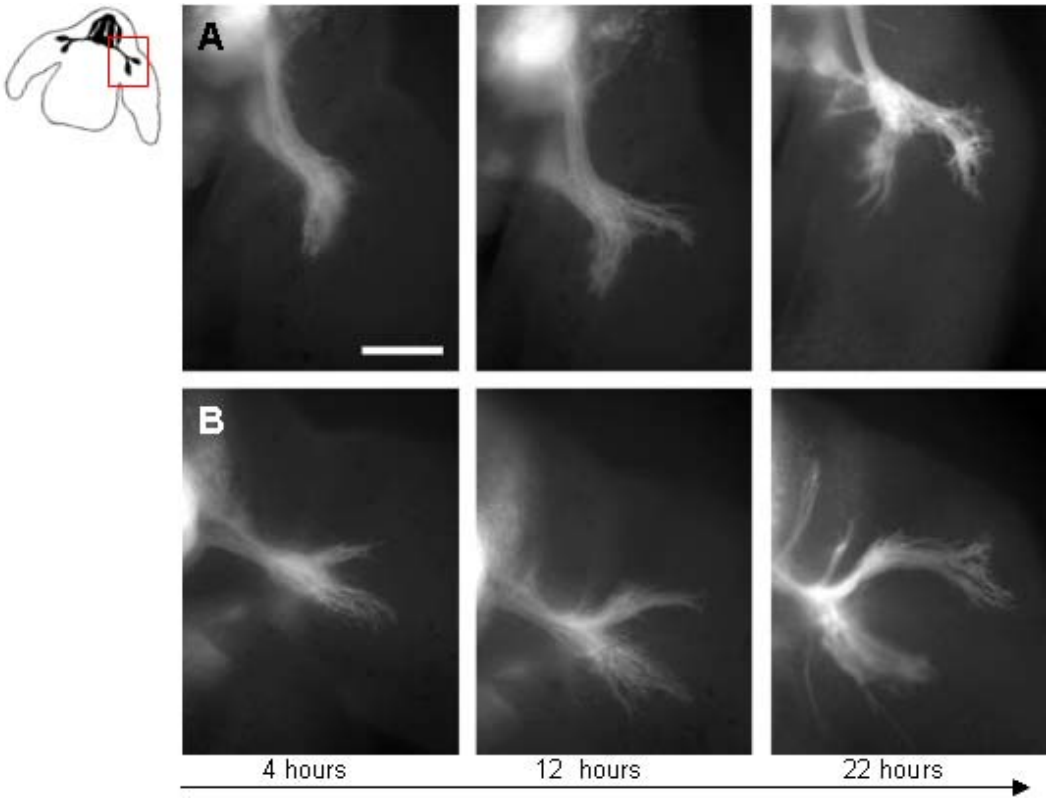

Fig. 3.4 - Spinal nerve outgrowth in two different slices (A and B) prepared from E10.5 tauGPF littermates. Slices prepared from separate embryos were photographed after 4, 12, and 22 hours in culture. The spinal cord and the DRGs are located on the left of each figure. Scale bar = 200 µm.

Almost all nerve branches showed a continuous outgrowth during the culture period. Although one might assume that nerves at the same developmental stage display similar outgrowth rates, there was no apparent direct correlation between various slices. Some nerves grew very slowly, some began slowly and sped up, while a third group grew at a moderate pace throughout the culture period (Fig. 3.5). This can be seen in the measurements of nerve outgrowth over the culture period (Fig. 3.5, A). There were nerves that showed a relatively stable outgrowth (Fig. 3.5, A: traces 1 and 4), and others with a variation of more than 30 µm/hour in their outgrowth rates (Fig. 3.5, B: traces 2 and 3).

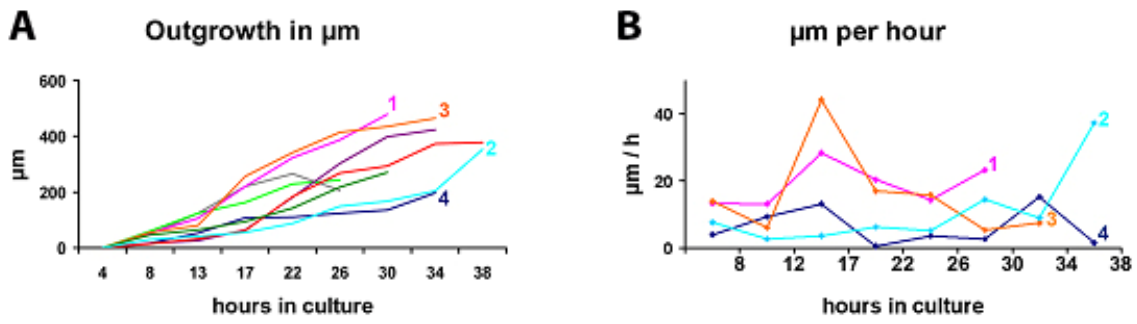

Fig. 3.5 - Spinal nerve outgrowth rates of cultured slices described in Fig. 3.4. **A:** Measurement of nerve outgrowth at indicated time points. Each line represents a nerve bundle in a different slice. **B:** The velocity of nerve outgrowth (µm/hr) was calculated for four spinal nerves.

Examination at higher magnification (Fig. 3.6) allowed the identification of the ends of individual axons with a morphology similar to that reported for growth cones *in vivo* (e.g. (Hollyday and Morgan-Carr 1995), but the depth of nerve growth in the tissue prevented adequate imaging of these structures with our epi-fluorescence microscopy equipment.

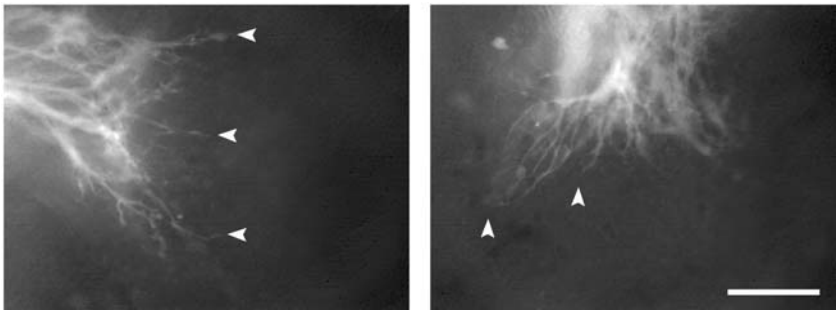

Fig. 3.6 - Higher magnification images of individual axon ends (arrowheads). Scale bar = 100 µm.

3.1.3.2 Axonal outgrowth in sagittal sections of the forelimb region

Since the transverse slices showed a robust outgrowth of the spinal nerves, the idea arose to also use sagittal slices of the forelimb region that would allow us to document the overall formation of the brachial plexus and the innervation of the forelimb.

Sagittal slices of E10.5 embryos were prepared with an effort on keeping as much of one lateral side as intact as possible. The outgrowth of the spinal nerves and the formation of the brachial plexus was documented taking images at regular time intervals (Fig. 3.7). At the beginning of the culture (4 h), the spinal nerve of thoracic level one had already reached the basis of the limb and started to defasciculate. At 16 hours in culture, the defasciculation of the spinal nerves of C7-Th1 continued and the first separation into the dorsal cord can be observed. During the next 20 hours the nerves continued with their outgrowth into the forelimb. In a small percentage of sections cultured for 48 hours spinal nerves had managed to innervate half of the forelimb (data not shown).

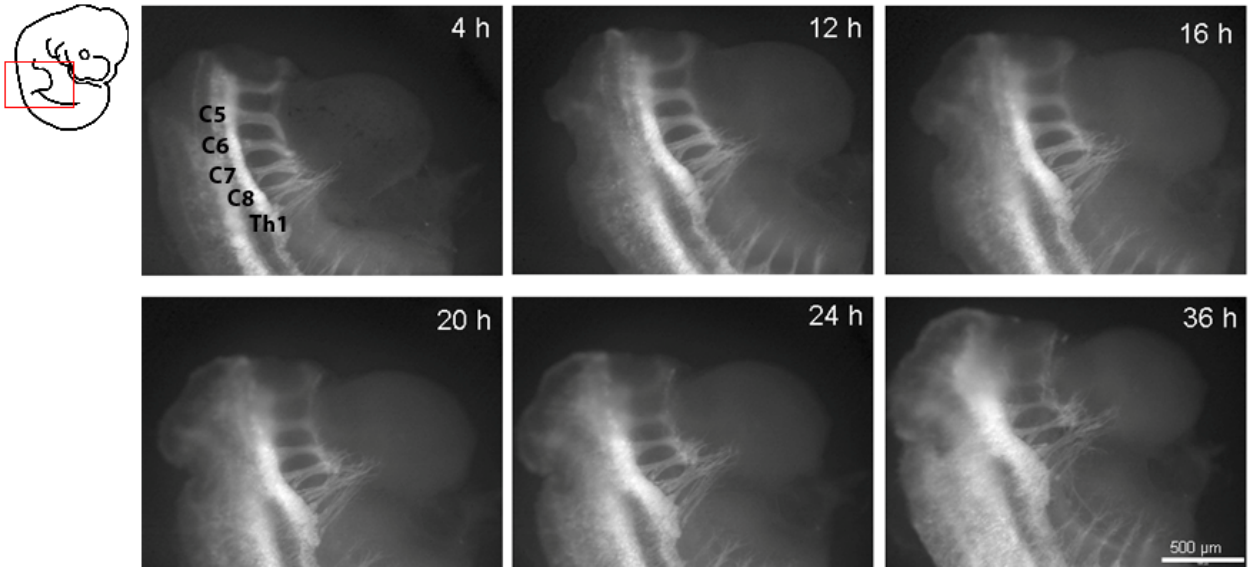

Fig. 3.7 - Sagittal section of trunk region containing the forelimb of E10.5 *tauGFP* embryo. The dorsal side is to the left. Scale bar = 500 µm.

Our results reveal a similar nerve outgrowth pattern including velocity in sagittal slice cultures compared to transverse ones.

3.1.4 Development of non-neural tissues within cultured slices

In order to show that the transverse slices retained a developmentally normal morphology over the course of the culture, we examined them with scanning electron microscopy (SEM) after 24 hours in culture (Fig. 3.8, A and B). Critical point drying was performed at the Institute for Physical Chemistry of the University of Heidelberg under the supervision of Vera Jakubick-Warnecke who also had the license to use the SEM.

The proximal half of the forelimbs, where the tissue had been cut (Fig. 3.8, A, arrows), had not been overgrown with epidermal cells and remained free of debris. The apical epidermal ridge could clearly be seen on the distal end of the forelimb (Fig. 3.8, A, arrowhead), the ventricles of the developing heart were clearly separated, and the spinal cord and DRGs retained their proper relationship to each other. In one third of the slices, the dorsal portion of the neural tube opened up after culture, as shown (Fig. 3.8, A). At higher magnification, the distal forelimb shows the characteristic morphology of the periderm cells that develop between E10.5 and E11.5 (Nakamura and Yasuda 1979), which have a flattened, longitudinally-oriented, polygonal shape (Fig. 3.8, B, asterisks). Developing periderm cells were also observed in toluidine blue-stained semithin transverse sections as a single layer of thin, elongated cells covering the epidermal layer beneath (Brachmann et al., 2007).

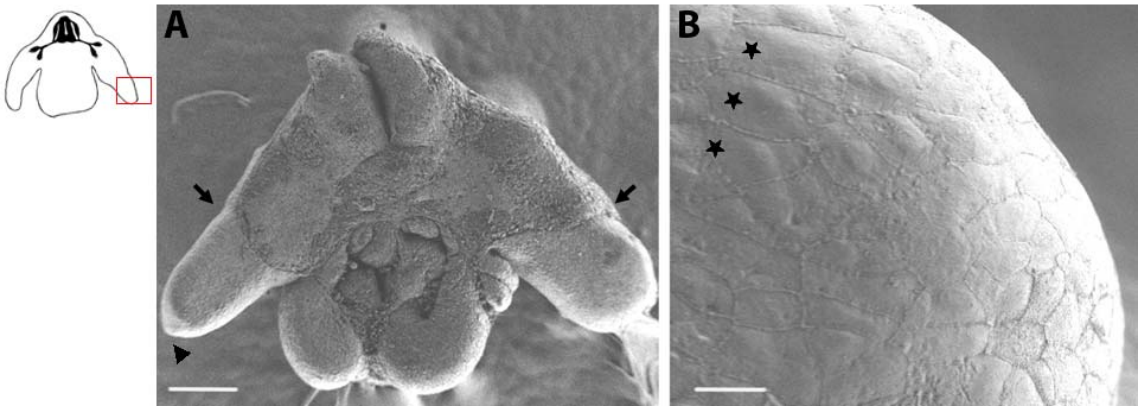

Fig. 3.8 - **A:** Scanning electron microscopy (SEM) image of an entire slice. The dorsal aspect of the slice is at the top of the figure. Arrows indicate where the forelimb was cut by the vibratome. Arrowhead indicates the apical ectodermal ridge of one forelimb. **B:** SEM image of the distal end of the forelimb in a slice. The proximal side of the forelimb is to the left. Stars indicate periderm cells. Scale bars = 200 µm in A, 20 µm in B.

At E11.5 the first signs of cartilage formation can be observed in the forelimb *in vivo* (Martin 1990), as revealed by Alcian blue stainings. As can be seen in slices prepared at E10.5, no Alcian blue staining was visible in the forelimb (Fig. 3.9, A). We compared the extent of staining of forelimbs from E11.5 embryos with slices of E10.5 embryos that had been cultivated for 24 hours. In both cultivated slices (Fig. 3.9, B) and the embryo (Fig. 3.9, C), a blue staining along the proximal central course of the forelimb could be observed, indicating that chondrogenesis had begun appropriately in the cultivated slices.

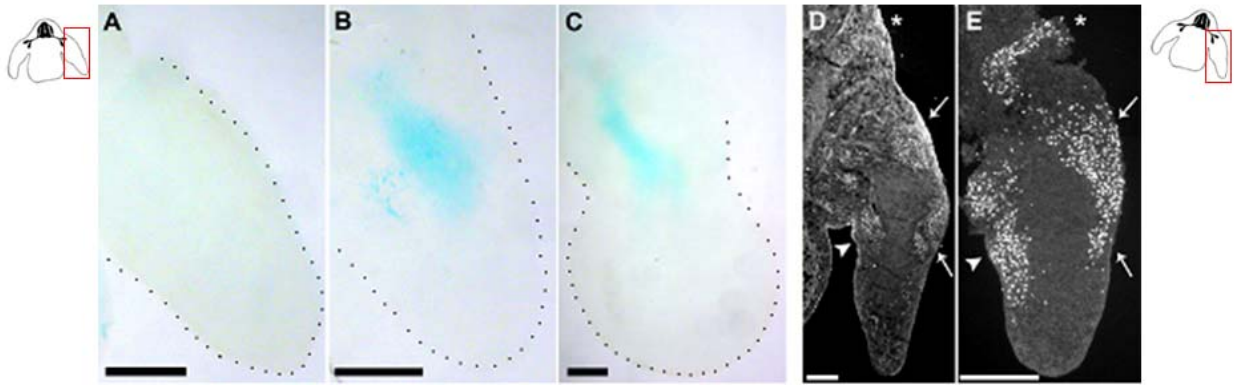

Fig. 3.9 - Development of non-neural tissues within embryonic slices prepared from E10.5 *tauGFP* embryos and cultivated for 24 hours. **A-C:** Chondrogenesis was examined using alcian blue stainings. **D-E**: Myogenesis was examined using an antibody recognizing MyoD1. **A:** A slice of a E10.5 embryo fixed immediately after cutting. **B:** A slice prepared of a E10.5 embryo cultivated for 24 hours. **C:** Forelimb of a E11.5 embryo. **D:** Cryosection of E11.5 embryo. **E:** Cryosection of an E10.5 embryo slice cultivated for 24 hours. The asterisk indicates the somatic myotome lateral to the DRGs. The lateral (arrows) and medial (arrowhead) myogenic compartments of the forelimb are indicated. Scale bars = 200 µm in A, B, C, and D, 500 µm in E.

During the same period of time, the first signs of myogenesis can be observed within the forelimb, as evidenced by the expression of the myogenic transcription factors MyoD1 and myogenin (Sassoon et al., 1989). We compared the spatiotemporal pattern of MyoD1 expression in forelimbs from E11.5 embryos (Fig. 3.9, D) with slices of E10.5 (Fig. 3.9, E) embryos that had been cultivated for 24 hours, using an antibody recognizing MyoD1. In both cases, large numbers of myogenic cells could be identified in the somitic myotome lateral to the DRGs, the lateral and medial myogenic compartments of the forelimb, and the nascent cardiac muscle in the developing heart.

Thus, our results reveal our slice culture system to present a suitable tool to monitor the time dependence of the axonal outgrowth pattern in relation to chondro- and myogenesis.

3.1.5 Quantification of cell death

In order to examine the viability of neurons and non-neuronal tissue in the slices over the culture period, Maya Shakèd-Rabi helped me to employ fluorescent-activated cell sorting (FACS) upon dissociated slices at progressive time points. Using FACS analysis we determined both the ratio between neurons (GFP-positive) and all other cell types (GFP-negative), and by adding the dye propidium iodide (PI) to the cell suspension we could determine the ratio between damaged or dead cells (PI-positive) and viable cells (PI-negative) (Fig. 3.10, A).

Slices were examined directly after the cutting procedure and after 24 and 48 hours in culture. Comparing the number of PI-positive and PI-negative cells within each population, a very low amount of cell death of both neurons and non-neuronal cells was observed at all three timepoints (Fig. 3.10, B). Our results show no significant difference in cell death between neurons and non-neuronal tissue in the cultured slices.

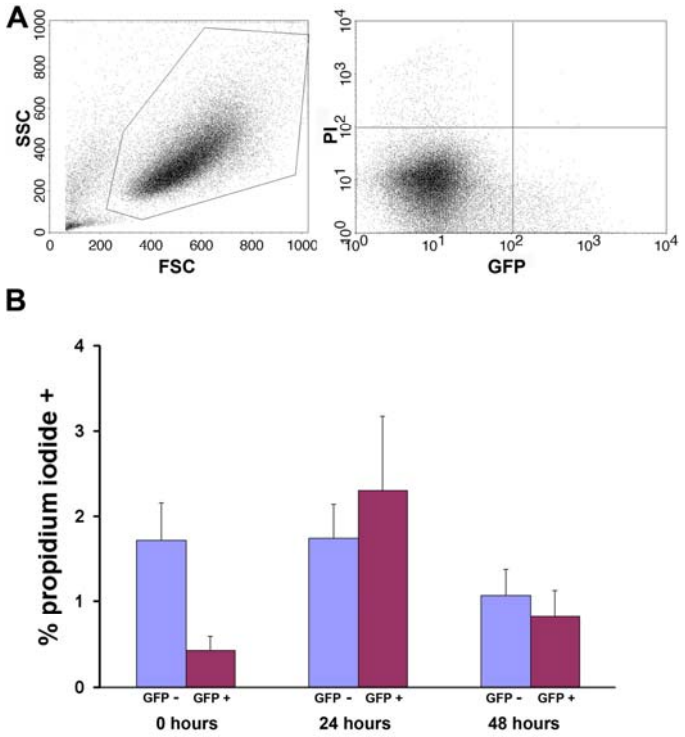

Fig. 3.10 - Analysis of cell death in slices prepared from E10.5 embryos by fluorescent activated cell sorting (FACS) analysis. Slices were trypsinized and dissociated into single-cell suspensions after the indicated culture times. Propidium iodide (PI) was added to assess the number of viable cells, and the cells were then analyzed for red (PI) and green (GFP) fluorescence by FACS. **A:** Representative FACS plots of slices cultured from *tauGFP* embryos. Forward (FSC) vs. sidescatter (SSC) is indicated on the left. The population of whole cells analyzed for red and green fluorescence is indicated by the gate. GFP vs PI fluorescence is indicated on the right. All cells to the right of the vertical line in this plot were judged to be GFP+ and therefore neurons. All cells above the horizontal

line in this plot were judged to be PI+ and therefore dead. **B:** The percentage of PI+ cells was calculated from the fraction of cells in the upper left (GFP-, non-neuronal) and upper right (GFP+, neuronal) quadrants of the scatter plot shown on the right (GFP vs. PI) in A, compared with the two respective PI-negative populations (SEM, n=3).

In order to compare the spatial pattern of apoptosis occurring within the cultured slices to the pattern in uncultured embryos, an antibody recognizing the cleaved, activated form of caspase-3 was utilized. In E11.5 embryos, almost all of the positive cells were found in the DRGs, but in the forelimbs of E11.5 embryos very little staining was seen (Fig. 3.11, A), as reported previously (Fernandez-Teran et al., 2006). In contrast, examination of slices prepared from an E10.5 embryo and cultivated for 24 hours displayed in contrast a higher amount of caspase-3 positive cells. Small numbers of activated caspase-3 positive cells could be found scattered throughout the forelimb, and a higher number of cells appeared in the DRG and the dorso-medial portion of the spinal cord (Fig. 3.11, B), indicating an enhanced apoptotic rate of sensory neurons in relation to culture time of tissue slices.

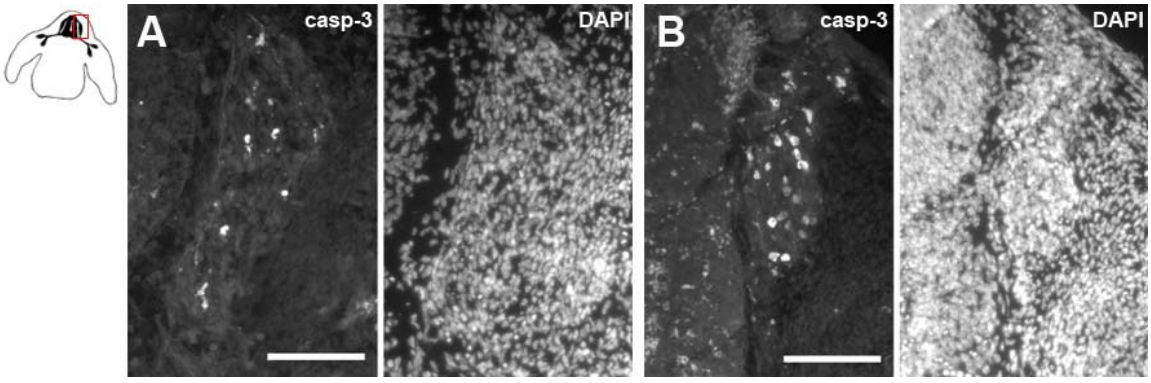

Fig. 3.11 - Apoptosis was examined using an antibody recognizing activated caspase-3 (casp-3). The DAPI staining reveals cell nuclei. **A:** Cryosection of E11.5 acute slice. **B:** A slice prepared of an E10.5 *tauGFP* embryo and cultivated for 24 hours. The transverse slice was then fixed and cryosectioned. Scale bars = 100 µm.

3.2 Analysis of the M22 mouse line

Several slices per *tauGFP* litter revealed continuous outgrowth that unfortunately could not be documented since the EGFP signal of outgrowing spinal nerves was too low to compensate for the deep tissue layers. Therefore we decided to import the M22 mouse line that was assumed to have stronger EGFP expression levels in neurons.

This mouse line has been generated by cloning an 8.8-kb stretch of genomic sequence surrounding the first exon of the *tau* gene, encompassing the *tau* promoter, the transcriptional start site, the first exon, and a portion of the first intron (Rittirsch and Tucker, Y.-A. Barde laboratory). This genomic sequence was then fused upstream of the EGFP gene. As the integration sites of the transgene were random, the expression of the endogenous *tau* gene is not affected.

3.2.1 Comparison of the EGFP expression in *tauGFP* and M22 embryos

Rederivation at the IBF Heidelberg was successful and provided 3 males that could be used as founders for the M22 colony. These animals were used to set up matings with C57Bl/6 females. A screen of the resulting litters revealed embryos which expressed EGFP throughout the central and peripheral nervous system and seemed to develop normally. Variations in development between embryos of one litter were limited and comparable to what we usually observed in other mouse lines (Kaufmann 2001). However, the embryonic development seemed to proceed slower at around E10.5, since M22 embryos were often smaller and not as developed as *tauGFP* embryos when dissected at the same time. To further compare the intensity of fluorescence between *tauGFP* and M22 embryos, homozygous *tauGFP* females were crossed to heterozygous M22 males, thus providing mixed litters consisting of embryos that are heterozygous for *tauGFP* and embryos that are in addition heterozygous for M22. In all screened E10.5 litters (>10), differences in the GFP intensity were obvious, particularly in the trigeminal ganglion and the trigeminal nerves (Fig. 3.12). Furthermore, there was a strong signal in the more caudal region of the hindlimbs that we had not observed so far at any developmental stage in *tauGFP* embryos.

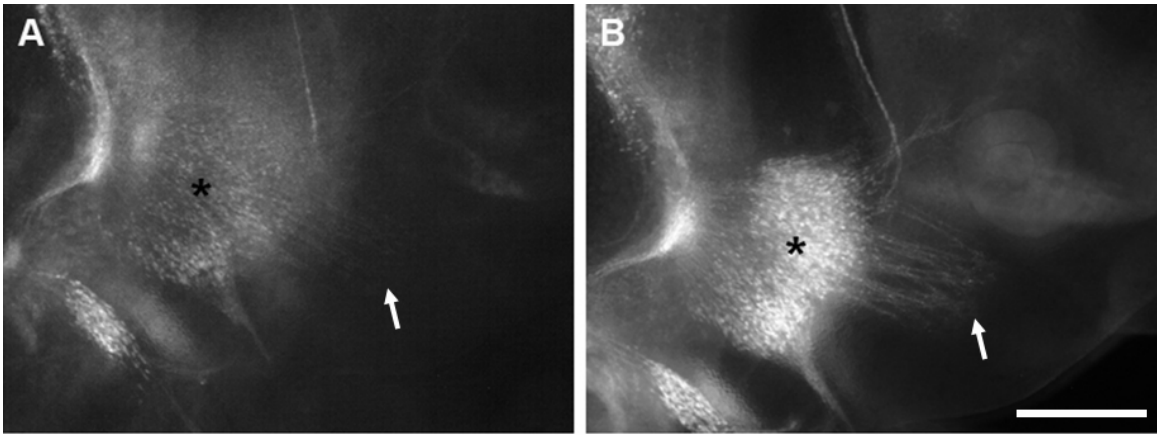

Fig. 3.12 - Trigeminal ganglions of E10.5 *tauGFP* (A) and *tauGFP*/M22 (B) embryos revealing differences in GFP intensity. **A:** Neurons of the trigeminal ganglion (asterisk) and the axons of the maxillary branch (arrow) reveal a weak GFP signal. **B:** Stronger signal of GFP in the trigeminal ganglion (asterisk) and the the maxillary branch (arrow). Scale bar = 500 μm.

3.2.2 Analysis of copy number using Southern blot analysis

Setting up the M22 colony, the aim was to generate a homozygous population of mice carrying as many copies of the *tauGFP* construct as possible. To identify these animals, we extracted DNA from tissue samples of *tauGFP* and M22 mice and compared the intensity of the bands achieved using Southern blot analysis (Fig. 3.13).

Using DNA samples of heterozygous and homozygous mice of the *tauGFP* mouse line as a reference, the analysis revealed a stronger EGFP expression for all M22 animal tested. The weakest signal is detected in lane 4 and 7, where DNA of heterozygous *tauGFP* animals was loaded. This signal corresponds to one copy of the construct. A stronger signal is apparent in lanes 5 and 6, which correspond to DNA samples of homozygous animals (two copies of the construct). Comparing the signal intensity of lanes 1, 2, 3, 8, 9, 10, and 11 with the intensity of the bands from the homozygous *tauGFP* mice, at least 6 M22 animals having three or more copies of the EGFP construct were found and these were kept to set up matings in the new colony. Offspring from matings between *tauGFP* mice and M22 mice are termed M22-*tauGFP* throughout this study.

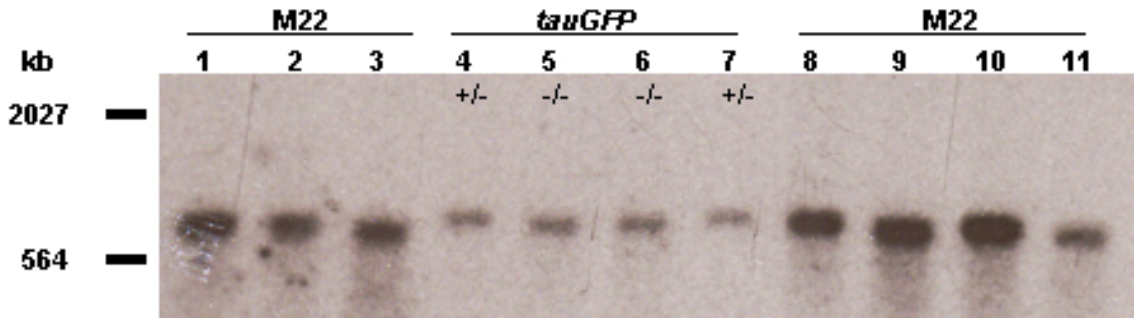

Fig. 3.13 - Southern blot analysis with DNA of M22 and *tauGFP* animals. Lanes 1-3 and 8-10 reveal a stronger signal than lines 5-6, meaning that 6 M22 animals have at least 3 copies of the *tauGFP* construct.

3.2.3 Analysis of the specificity of the EGFP expression pattern in M22-*tauGFP* embryos

Having seen a stronger EGFP signal looking at M22-*tauGFP* embryos with an epi-fluorescent microscope and having shown a higher construct number by Southern blot analysis, a third step during the analysis of this mouse line was to characterize the specificity of the GFP expression using immunohistochemistry. Applying antibodies against GFP (although the signal of the endogenous GFP would have been sufficient) and class III ß-tubulin (TuJ1) on transverse and sagittal cryosections of E10.5 and E12.5, a clear colocalisation of both antibodies was observed, indicating a highly specific GFP expression in the nervous system (Fig. 3.14).

In transverse sections of E10.5 embryos at the forelimb level, GFP is expressed by neurons located in the mantle zone of the neural tube, by the motorneurons located ventrally in the neural tube, by the sensory neurons in the DRGs, by neurons located in the sympathetic ganglia, and GFP signal is also detected along the spinal nerves. Since no structure was labeled by only one antibody, this mouse line was used in our further time lapse imaging experiments.

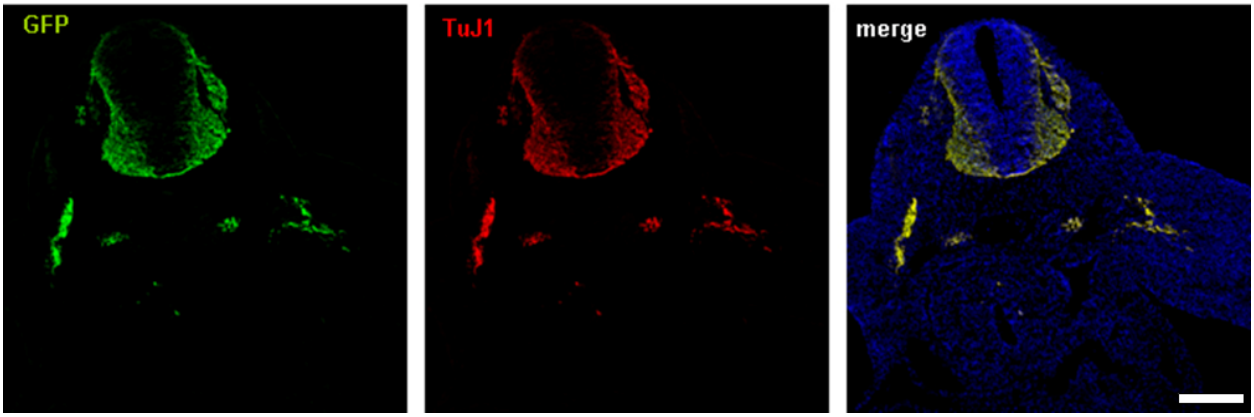

Fig. 3.14 - Colocalization of GFP and classIII ß-tubulin (TuJ1) in transverse cryosections at the forelimb level of E10.5 M22-*tauGFP* embryos. Scale bar = 200 µm.

3.2.4 Time-lapse imaging of M22-*tauGFP* spinal nerve outgrowth

Using vibratome slices of E10.25 M22 embryos, it became easier to follow nerve outgrowth at low magnifications. The stronger GFP signal also allowed to image outgrowth in deeper tissue regions, where imaging on slices of *tauGFP* has been impossible with our equipment. The innervation pattern of the forelimb revealed in M22-*tauGFP* slices is similar to that observed in the slices of the *tauGFP* mice (Fig. 3.15). The spinal nerves separate to form the dorsal and the ventral cord, a process that is accompanied by the defasciculation of the nerve bundles (Fig.3.15, 2-6 hours). Both the ventral and the dorsal cord continued their outgrowth during the following hours in culture and innervated their appropriate target areas.

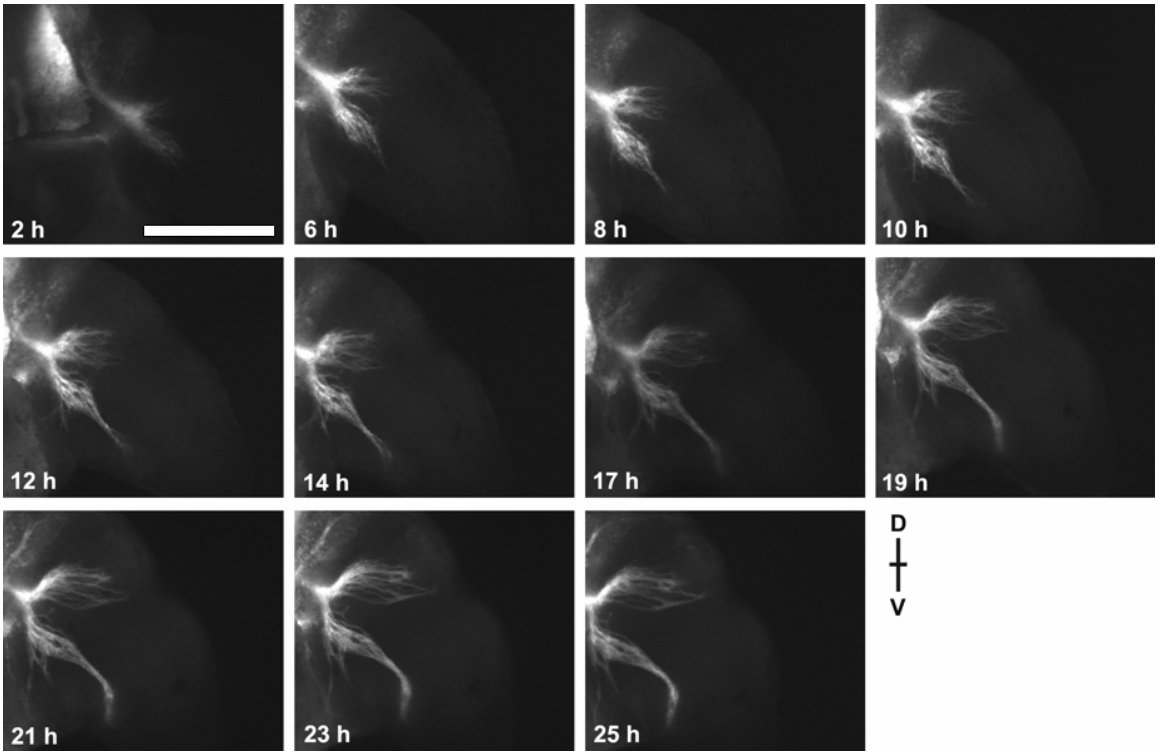

Fig. 3.15 - Spinal nerve outgrowth in a transverse slice prepared from E10.25 M22-*tauGFP* embryo. The dorsal side of the embryo is at the top of each figure, the spinal cord and DRG are located on the left of each figure. Hours spent in culture are indicated in the bottom left of each image. Scale bar = 500 µm.

3.3 The semaphorin3A deficient mouse

The use of this mouse model for the described slice culture system offers the opportunity to examine paradigmatically the effect of mutations in specific genes during the development of peripheral nerves. As an example, we have investigated the role of the gene encoding Semaphorin3A (*Sema3A*) in PNS development. As mentioned in the introduction, Sema3A is a secreted protein within the semaphorin gene family that acts as a chemorepulsive cue throughout the developing central and peripheral nervous system (Pasterkamp and Kolodkin 2003). Sema3A binds to the receptor complex neuropilin-1 / plexinA to induce a signalling cascade leading to cytoskeletal rearrangements and growth cone collapse. In the developing forelimb, *Sema3A* is expressed in tissues surrounding the outgrowing spinal nerves (Wright et al., 1995). Elimination of either *Sema3A* (Taniguchi et al., 1997; White and Behar 2000) or its receptors neuropilin-1 (Kitsukawa et al., 1997) and plexin-A4 (Suto et al., 2005; Yaron et al., 2005) leads to promiscuous outgrowth of spinal nerves into normally non-permissive regions.

Performing whole mount stainings on *tauSEM* litters with an antibody against neurofilamentM we observed a premature outgrowth in the forelimb of E11.5 Sema3A mutant embryos (Fig. 3.16).

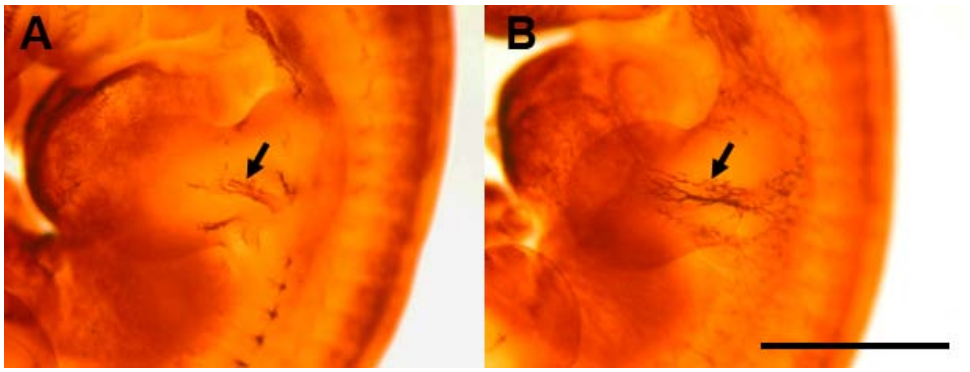

Fig. 3.16 - Promiscuous outgrowth of spinal nerves into the forelimb revealed by anti-neurofilamentM staining (anti-2H3)(arrows). Forelimbs of littermates of E11.5 tauSEM embryos. **A:** *tauSEM* control **B:** *tauSEM* (Sema3A mutant). Scale bar = 1 mm.

3.3.1 Imaging of peripheral nerve outgrowth in the targeted *Sema3A* mouse mutant

In order to perform timed imaging of embryonic slices derived from mice lacking *Sema3A* (Behar et al., 1996), we crossed the *Sema3A* knockout mouse to the *tauGFP* line, resulting in *tauSEM* mice. Throughout this study we will refer to animals that are heterozygous for the *Sema3A* mutation as *tauSEM*$^{+/-}$ and to animal that are homozygous for the *Sema3A* mutation as *tauSEM*$^{-/-}$. As reported by White et al. previously (White and Behar 2000), at E10.5 we could clearly observe premature outgrowth and a strong defasciculation of spinal nerves in *tauSEM*$^{-/-}$ embryos, compared to GFP expressing littermates that were wild type or heterozygous for the *Sema3A* mutation (Fig. 3.17).

At the beginning of the imaging series, slices from *tauSEM*$^{-/-}$ embryos showed an approximately 12-hour advance in spinal nerve outgrowth compared to *tauGFP* or *tauSEM*$^{+/-}$ heterozygous littermates (Fig. 3.17, 9h). In the *tauSEM*$^{-/-}$ embryos, not only had the spinal nerves prematurely formed trunks and fasciculated into dorsal and ventral cords, but also the ventral cord had branched and the main myotomal rami had already developed. As the spinal nerves in the *tauGFP* slices began their outgrowth (Fig. 3.17, 17 h and 25 h), the nerves in the *tauSEM*$^{-/-}$ slices elongated much slower (Fig. 3.17, 13 h, 17 h, 25 h). After 25 hours of culturing the *tauGFP* and *tauSEM*$^{-/-}$ slices displayed an equivalent progress in nerve outgrowth (Fig. 3.17, 37 h). Comparing the *tauSEM*$^{-/-}$ slices at the beginning and end of culture revealed that the nerve branches at the end of the culture did not appear as defasciculated as at the beginning of culture, resembling more the *tauGFP* slices (Fig. 3.17, 37 h).

Our results clearly show and confirm earlier results in *Sema3A*$^{-/-}$ mice. Not only could the premature outgrowth and the defasciculation of spinal nerves be observed, but also first signs of a correction mechanism might have been visible in the *tauSEM*$^{-/-}$ slices (White and Behar 2000).

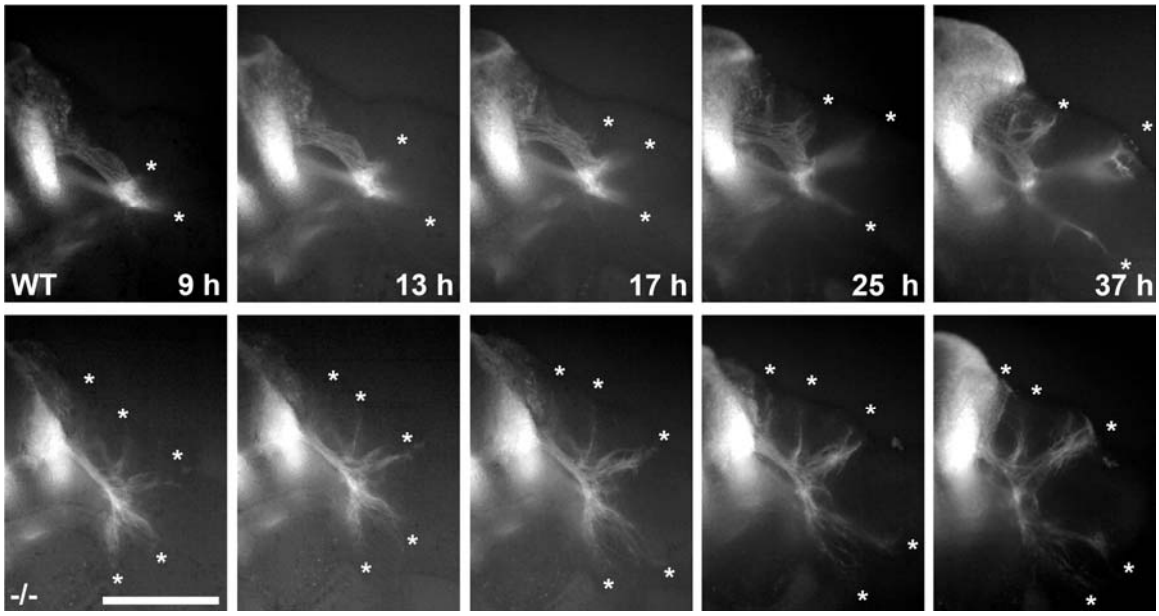

Fig. 3.17 - Spinal nerve outgrowth in slices prepared from a litter of E10.5 *tauSEM* embryos **Upper panel:** *tauSEM* control, **lower panel:** *tauSEM*$^{-/-}$ The dorsal side of the embryo is at the top of each figure. Hours spent in culture are indicated in the bottom right of each image. Asterisks indicate the ends of the outgrowing spinal nerves, only on the right side of the slice. Scale bar = 500 µm.

3.3.2 Occurrence of ectopic cells in *tauSEM* embryos

During time-lapse imaging of spinal nerve outgrowth of *tauSEM* litters, in a subset of slices not only a premature outgrowth of spinal nerves, especially of those originating from the dorsal cord was observed, but also thickenings along their course revealing a speckled fluorescent signal (Fig. 3.18). While after 12.5 hours in culture only one major cluster was detected along the dorsal cord (Fig.3.18, 12 h (asterisk)), there appeared at least two more over the next 8 hours (Fig. 3.18, 12.5-20 h (asterisks)). Performing PCR to genotype tissue samples taken from slices where these clusters have been observed proved that only slices of *tauSEM*$^{-/-}$ embryos revealed this speckled signal.

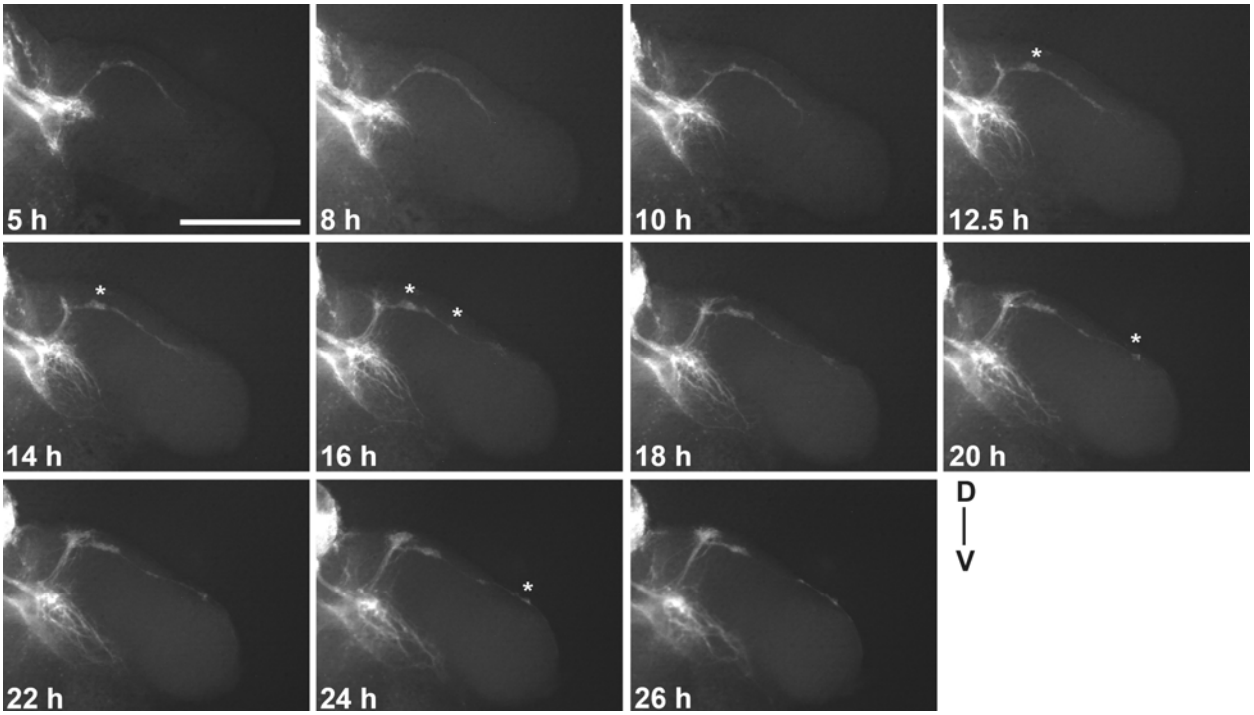

Fig. 3.18 - Time-lapse series of spinal nerve outgrowth in a transverse slice of a *tauSEM*$^{-/-}$E10.5 embryo. Scale bar = 500 µm.

Although premature outgrowth and defasciculation of spinal nerves have been described for Sema3A mutant mouse lines as well as for mouse lines that have mutations in one of the receptors, none of these articles presented any data about the clusters observed in our slice cultures (Behar et al., 1996; Taniguchi et al., 1997). To exclude that this might be a tissue culture artifact, we prepared vibratome sections of E10.5 and E11.5 littermates and compared *tauGFP* or *tauSEM*$^{+/-}$ with *tauSEM*$^{-/-}$embryos. As mentioned above, the spinal nerves of *tauSEM*$^{-/-}$ had grown out into areas of the forelimb where they are not found in heterozygous or wildtype littermates. Astonishingly, the clusters were constantly formed and detected in acute slices, cut from E10.5 and E11.5 old embryos (Fig. 3.19).

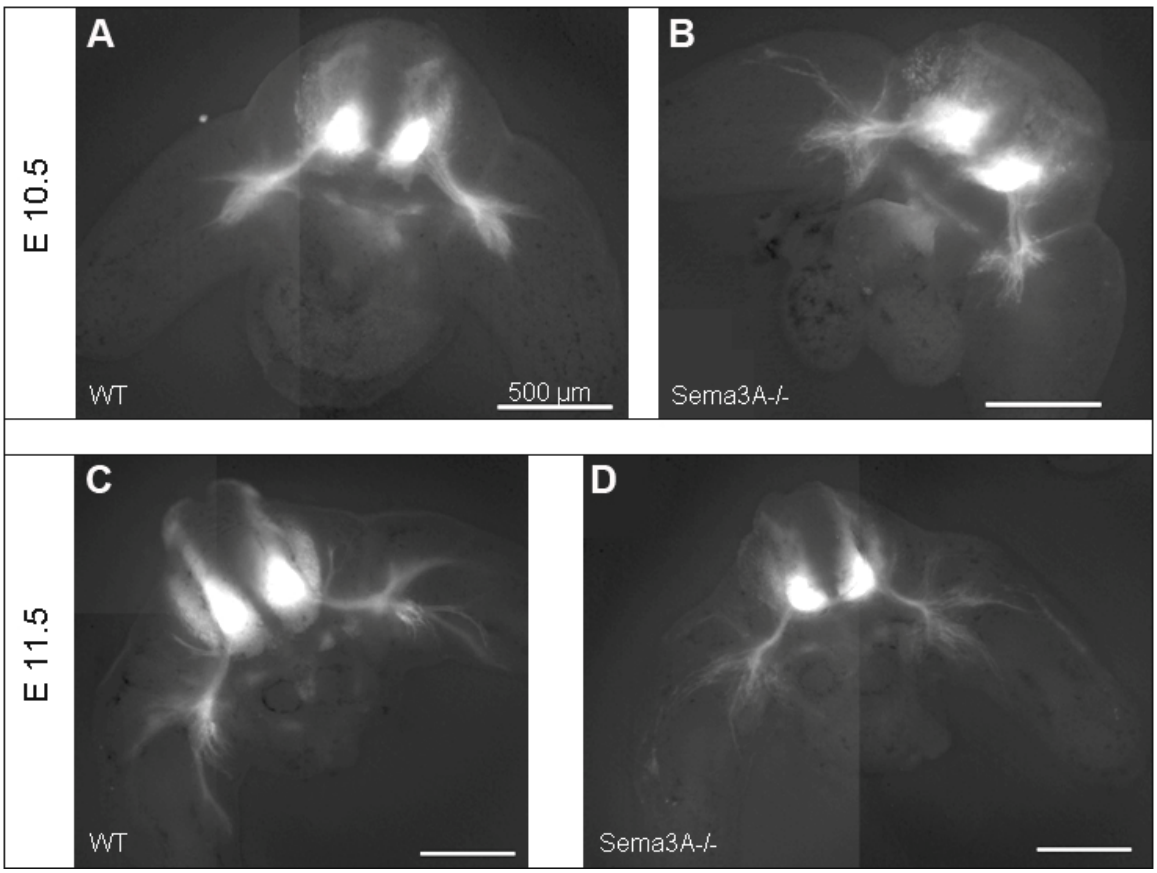

Fig. 3.19 - Spinal nerve outgrowth in acute transverse slices prepared from *tauSem* litters of E10.5 (A and B) and of E11.5 (C and D). WT = *tauGFP* or *tauSEM*$^{+/-}$; *Sema3A-/-* =*tauSEM*$^{-/-}$. Scale bar = 500 µm.

In order to document the clusters at a higher resolution, confocal microscopy was employed. Cultivated 350 µm transverse slices of E10.5 *tauSEM*$^{-/-}$ embryos that had been used for imaging were fixed and stained with a fluorescent antibody against GFP to ensure high fluorescent intensity. Fast scans through the slices were performed to establish an overview of the neural tube and the spinal nerves (Fig 3.20, A, D), followed by Z-stacks of the layers the spinal nerves were located in. Using higher resolution (Fig. 3.20, B), the clusters could be visualized as cell aggregates.

As the GFP expression in the *tauSEM* mouse line originated from the *Mapt* locus, these cells were most likely postmitotic neurons. Taking advantage of the confocal microscope and screening also regions closer to the neural tube, further GFP positive cells could be located along the ventral roots as well as lateral to the DRGs (Fig. 3.20, C, E, F). Interestingly, all detected cells were found to be in contact with fascicles. To clarify the character of these ectopic cells we

continued with cryosections and immunohistochemistry prepared from *tauSEM*$^{-/-}$ embryos of E11.5.

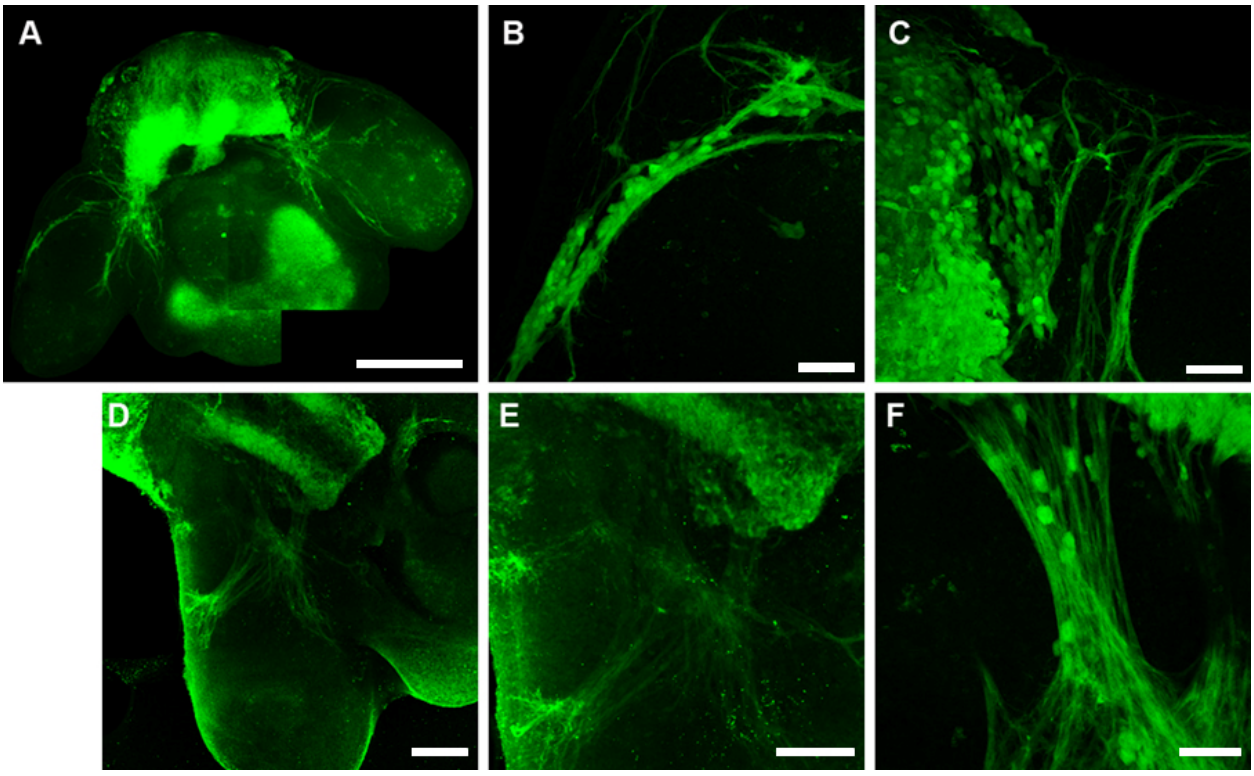

Fig. 3.20 - Z-projections of transverse slices of E10.5 *tauSEM*$^{-/-}$ embryos cultivated for 24 hours. GFP staining revealing defasciculated spinal nerves and nerve bundles innervating improper areas. **A and D**: Low magnification images of slices. Dorsal is located up. **B-C:** Higher magnification of areas in A. **B:** Cells positive for GFP are adjacent to nerve bundles of the dorsal cord. **C:** Sensory neurons of a DRG and misprojecting nerve bundles out of the DRG and parallel to the DRG. **E:** Aspect of D at higher magnification with ventral and dorsal roots of several segments. **F:** Aspect of E at higher magnification showing dorsal and ventral roots forming the nascent brachial plexus. Several cells positive for GFP are located outside the DRG and the spinal cord. Scale bars = 200 µm in A, D and E, 50 µm in B, C and F.

3.3.3 Characterisation of ectopic cells in *tauSEM*$^{-/-}$ animals

In order to characterize the cells detected in ectopic positions of the lateral mesenchyme and the developing forelimb (Fig 3.21, B), stainings using various antibody combinations were performed upon cryosections of E11.5 old Sema3A$^{-/-}$ and tauSem$^{-/-}$ embryos.

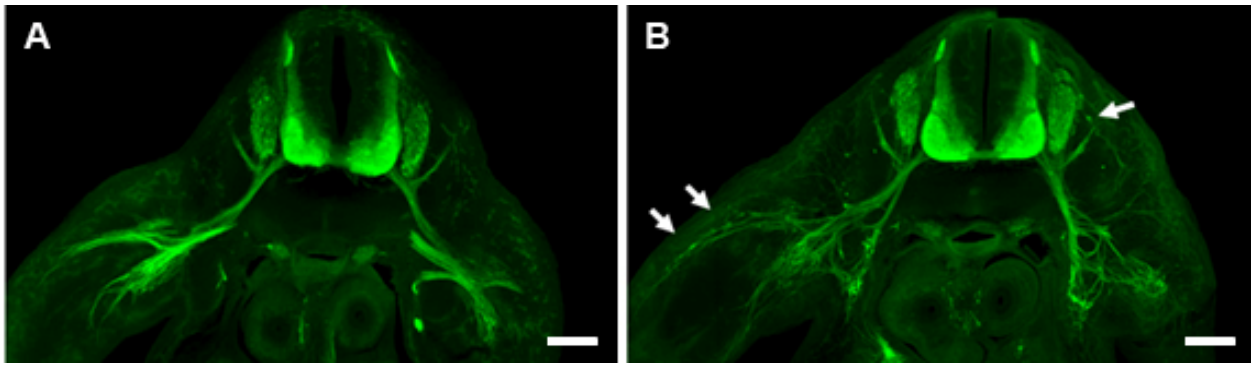

Fig. 3.21 - Z-projections of transverse slices of E11.5 *tauSEM* embryos. **A**: Section of a control embryo. **B**: Section of a *tauSEM*$^{-/-}$ embryo, revealing ecotopic GFP positive cells in the lateral mesenchyme and along the dorsal cord of the forelimb (arrows). Scale bar = 200 µm.

In a first step the neuronal character was addressed, followed by stainings to control the developmental stage of these cells.

3.3.3.1 Ectopic cells are of neuronal character

Since all of the detected ectopic cells expressed GFP, it seemed to be likely that the observed cells were postmitotic neurons. The two main candidate populations in the peripheral nervous system are sensory and sympathetic neurons. Also knowing that a lack of Sema3A signaling via the neuropilin1 receptor can lead to a displacement of sympathetic neurons and their precursors (Kawasaki et al., 2002), the first stainings were planned to localize these two populations using tyrosine hydroxylase (TH) and the brain-specific homeobox/POU domain protein 3A (Brn3a). TH is the rate limiting enzyme in catecholamine biosynthesis, and a classical marker for cells of the sympathoadrenal cell lineage. Brn3a is a transcription factor that can be used to detect early postmitotic CNS-neurons, but also sensory neurons and their neural precursors (Fedtsova and Turner 1995). To be able to differentiate between postmitotic sensory neurons and putative neuronal precursors, a co-staining with anti-TuJ1 was performed.

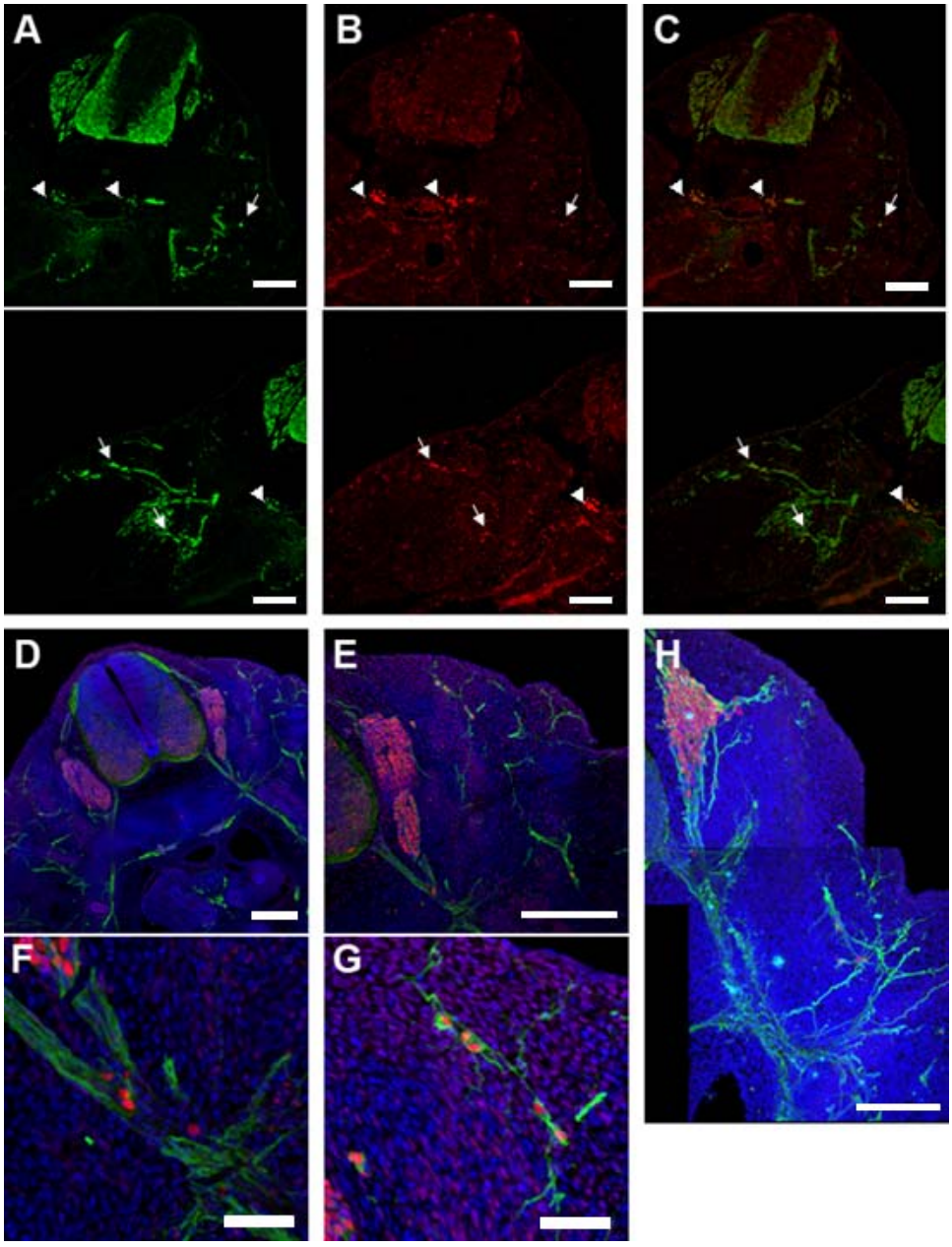

Fig. 3.22 - Ectopic cells in transverse sections of E11.5 *tauSEM*$^{-/-}$ embryos are positive for TH and Brn3a. The dorsal side is on all images at the top of the panel. **A-C:** Co-staining with anti-GFP and anti-TH. Sympathetic ganglia stained by both antibodies are indicated by arrowheads, ectopic cells revealing colocalization are indicated by arrows **D-H:** Co-staining of anti-Brn3a and anti-TuJ1. **D:** Overview of the areas presented in E-G. **E:** Ectopic cells located laterally to the DRG and in the ventral root of the spinal nerve are TuJ1 and Brn3a positive. **F-G**: Higher magnification of relevant areas in E. **H:** Brn3a and TuJ1 positive cells are also located along nerve fascicles in the proximal region of the limb. Scale bars = 200 µm in A, B, C, D = 100 µm in E, H, 50 µm in F and G.

The staining with anti-TH on E11.5 *tauSEM*$^{-/-}$ cryosections of the forelimb region revealed cells positive for both TH and GFP that were not located in the sympathetic ganglia, but rather laterally and ventrally to them (Fig. 3.22, A, B, C). The positions at which these cells were found are consistent with the data presented by Kawasaki and coworkers., confirming that Sema3A signaling plays a role during patterning of the sympathetic nervous system (Kawasaki et al., 2002).

The staining with anti-Brn3a and anti-TuJ1 on cryosections of E11.5 *tauSEM*$^{-/-}$ embryos revealed a normal expression of Brn3A in the ventral spinal cord and the DRGs. However, there were additional Brn3a positive cells located laterally (Fig. 3.22, E, G, H) and ventrally (Fig. 3.22, F) to the DRGs, as well as in the proximal part of the forelimb (Fig.3.22, H). Monitoring the dorsal cords in *tauSEM*$^{-/-}$ sections, no signal of Brn3a could be detected, indicating that the more distally located cells had to be a different cell population. All of the Brn3a positive ectopic cells also expressed TuJ1, indicating that these cells are postmitotic neurons.

3.3.3.2 Two distinct populations of ectopic cells are detected in *tauSem* embryos

Under my supervision, Silke Herzer performed co-stainings with anti-TH and anti-Brn3a antibodies during her bachelor thesis on the characterization of these cells and could show that there are two distinct cell populations which are located ectopically in the trunk region of the forelimb of E11.5 *tauSEM*$^{-/-}$ embryos (Fig. 3.23).

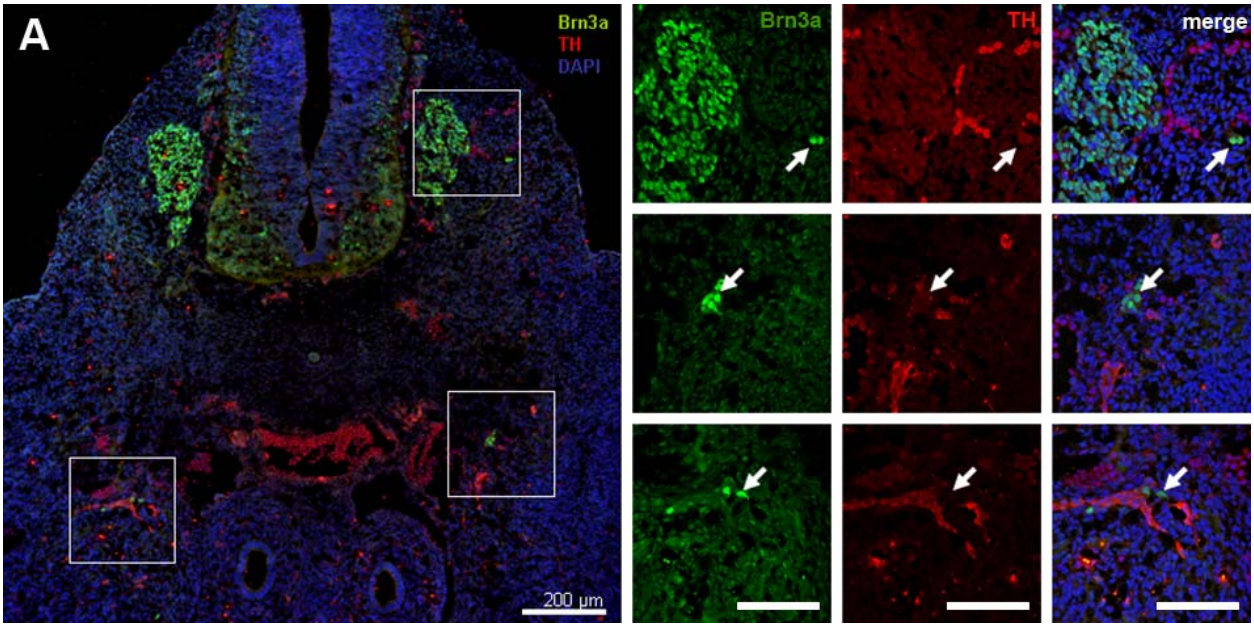

Fig. 3.23 - Two distinct populations of ectopic cells exist in transverse slices of E11.5 *tauSEM*$^{-/-}$ embryos. Co-staining with anti-Brn3a and anti-TH revealed two separate populations of ectopically located cells. Scale bar = 200 µm in A, 100µm for magnifications.

3.3.3.3 Ectopic cells are not proliferating

Although all markers used so far provided evidence that the ectopic cells were postmitotic neurons and even committed to either the sensory or the sympathoadrenal lineage, we wanted to ensure that we had not missed a cell population comprising neural precursors. Combining stainings for the cell proliferation marker Ki-67 and Brn3a, cells that were still in a state of proliferation and positive for Brn3a should colabel with Ki-67. In any slice that revealed ectopically located cells (Brn3a positive) no colocalization for these two markers was detected (Fig. 3.24). This result is in accordance with stainings performed for anti-PH3, an additional proliferation marker (data not shown).

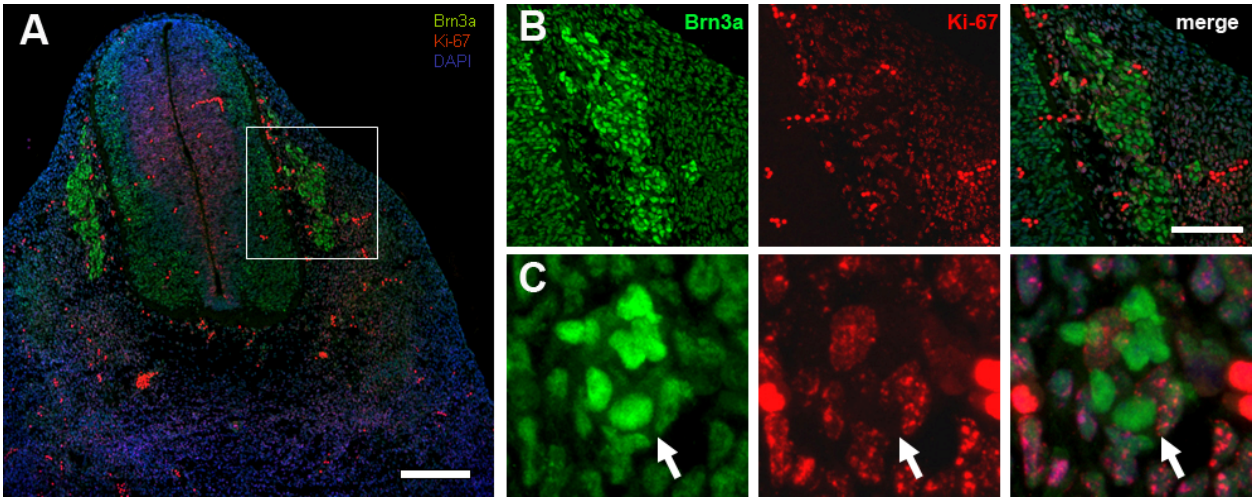

Fig. 3.24 - Transverse slice of E11.5 *tauSEM*$^{-/-}$ embryo stained with anti-Brn3a, anti-Ki67 and DAPI as nuclear marker. **A:** Low magnification. **B**: Higher magnification of the DRG as indicated by the white box. **C**: Cell cluster that was located on the right side of the DRG in B. Scale bars = 200 µm in A and 100 µm B.

3.4 Effect of Sema3A on neural crest cells

Both the sensory and the sympathoadrenal lineage of neurons are derived from migrating trunk neural crest cells, that delaminate from the dorsal neural tube and start their migration ventrally to eventually form the sympathetic and the dorsal root ganglia. Several papers were published recently, describing the effect a loss of Sema3A signaling has on positioning cranial sensory neurons (Schwarz et al., 2008) as well as on ectopic neuronal differentiation in the trunk region of the mouse (Schwarz et al., 2009). However, the only direct effect of Sema3A on neural crest was shown in neural crest cultures of chick (Eickholt et al., 1999). To investigate if Sema3A signaling has a repulsive effect on neural crest cells, tissue cultures using neural tube explants were set up and treated with various concentrations of Sema3A.

Since Sema3A is a secreted protein, a common method to generate it, is to transfect HEK293 cells and harvest it from the medium (Puschel et al., 1995). To determine the appropriate amount of HEK cell medium needed to produce a repulsive effect on cultured cells, DRG explant cultures were prepared as reference cultures. DRG explant cultures have been used to test for repulsive and attractive guidance cues over the last decades and their sensory neurons have been shown to be responsive to Sema3A (Messersmith et al., 1995; Masuda et al., 2003).

Collapse assay to analyse the repulsive effect of Sema3A on neural crest cells

Neural tube segments of E 9.0-9.75 embryos were cultured for 20-24 hours to allow adhesion and radial migration of neural crest cells away from the explant. After 6 hours in culture, the first migrating cells were observed and after 24 hours the neural tube explant was surrounded by cells that adhered to the coverslips and migrated away from the neural tube in a radial fashion (Fig. 3.25, A).

Stainings using an antibody against neurotrophin receptor p75 that were performed on neural crest explant cultures showed that about 90% of the migrating cells are positive for this marker, indicating that the cells are either neural crest cells or neural progenitors (Fig. 3.25, B and C).

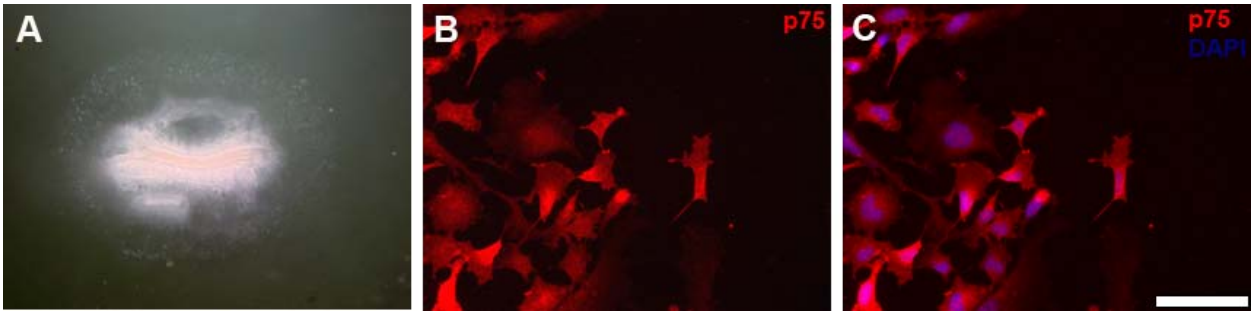

Fig. 3.25 - Neural crest cultures. **A:** Neural tube explant surrounded by migrating cells. 48 hours in culture. **B:** Staining with anti-p75 reveals migrating neural crest cells or neural progenitors. **C:** DAPI was used as a cell nuclei marker. Scale bar = 100 µm.

Applying Sema3A to neural crest cultures did not produce a significant retraction of filopodia or lamellipodia, although the same concentrations applied to DRG cultures lead to growth cone collapse and axon retraction (Fig. 3.26). Documenting the neural crest migration using a time-lapse series and adding commercially produced Sema3A in concentrations of 10-100 µg/ml, also no retraction or cell detachment could be observed.

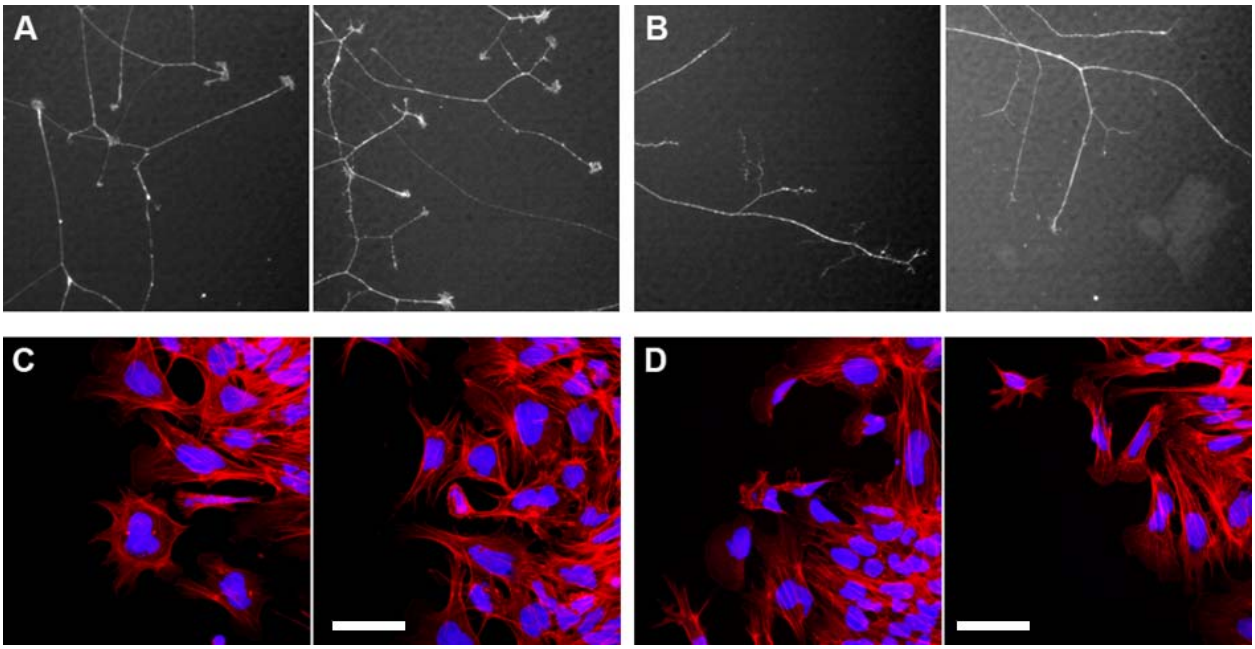

Fig. 3.26 - Dorsal root ganglion (DRG) and neural tube explant cultures. **A-B:** DRG cultures of E13.5 embryos. **A:** Control cultures treated with HEK cell medium of cultures transfected with pEGFP. **B:** Cultures treated with 50 and 100 µl HEK cell medium containing Sema3A. **C-D:** Neural crest cell after cultivation for 20 hours. No significant difference could be observed between control and Sema3A treated cultures. **C:** Neural crest cell cultures treated with medium of pEGFP transfected HEK cells. **D:** Neural crest cell cultures treated with HEK cell medium containing Sema3A. Scale bars = 50 µm in C and D.

4 Discussion

This thesis presents the successful establishment of a slice culture system that allows the observation of spinal nerve outgrowth as it proceeds *in situ*. Employing mice whose developing nervous system is labeled by EGFP, we could document a forelimb innervation pattern that resembles the endogenous one in regard to the target areas and time. Furthermore, an analysis performed on non-neural tissues revealed that epidermal development, chondrogenesis, and myogenesis occur during the cultivation time at the correct stages of embryonic development *in situ*. In order to image axonal outgrowth at a higher resolution, a mouse line expressing a stronger EGFP signal was imported and analyzed. Parallel to that, we took advantage of our slice cultures by imaging the promiscuous outgrowth of spinal nerves in Sema3A mutant embryos. Applying the slice culture system on these mutants let us detect misplaced cells that had not been described up to then.

4.1 The slice culture system to image neuronal outgrowth

Most of the molecular pathways involved in axonal guidance have been elucidated on cell cultures *in vitro*. However, the natural environment in which axons grow is much more complex and can hardly be reproduced *ex vivo*, especially for studying nervous system formation. It is therefore important to manipulate nerve outgrowth *in situ* and to observe the effects of such manipulations in real-time, using similar techniques to those used very successfully in *in vitro* experiments. Transverse sections prepared from chick embryos proved to be a powerful tool to investigate spinal nerve outgrowth and elucidated crucial molecular mechanisms in pathfinding decisions. Their disadvantage was that the outgrowing nerves had to be labeled after the culture period, or stained with a fluorescent dye when the slices were prepared in order to distinguish nerves from their surrounding tissue. Using a transgenic mouse line (*tauGFP*) expressing EGFP in the postmitotic neurons of the central and peripheral nervous system (Tucker et al., 2001) and preparing slices that comprise enough tissue to support the outgrowth of spinal nerves, provided a powerful mammalian system that allowed the reproduction of spinal nerve outgrowth similar to *in vivo*. Furthermore, the system offered the possibility to elucidate the effects of the spatiotemporal expression pattern of attractants and repellents on axonal outgrowth and pathfinding using different mutant mouse models.

4.1.1 Improvements upon slice cultures and establishment of a time lapse imaging system

The aim of this thesis was to establish a slice culture system that allows one to reproduce and analyze the forelimb innervation in mouse *ex vivo*, and to document the development of this innervation pattern performing time-lapse imaging. Having created a functional stable system, several questions in regard to spinal nerve outgrowth were planned to be addressed:

1. Do mouse spinal nerves reveal "waiting period" events as it was described for chick (Tosney and Landmesser 1985; Wang and Scott 2000)?
2. Can outgrowth rates and velocities for distinct nerves and their branches be compared?
3. Do motor and sensory neurons respond to short or medium range cues as it is described for cell culture systems?
4. Do spinal nerves of tauSEM homozyogous mutant embryos show key features that had been found in Sema3A mutant embryos of the corresponding embryonic age (Behar et al., 1996; Taniguchi et al., 1997)?

In order to reproduce an endogenous developmental pattern of the limb innervation, two issues seemed to be most critical. One was to find a slicing technique that would cut fast enough, but on the other hand still gentle enough, to prepare high quality slices of one litter in a short amount of time. The second was to guarantee stable, standardized tissue culture conditions on the stage itself, spending as few money as possible.

Preparing slices with a vibratome (Mikrom HM 650 V) fulfilled all the demands. The slicing conditions were easily reproducible. In case litters contained only embryos with the same genotype, several embryos could be cut at the same time, or for varying genotypes could be cut separately from each other.

Setting up the equipment needed at the microscope was more challenging, dealing with an upright microscope and investing the time needed to produce the heating device and the macrolon box. The final success came when a second internal heating system, originally delivered for an inverse microscope, was employed.

4.1.2 Imaging peripheral nerve outgrowth in *tauGFP* transverse slices

In slices of E10.25 and E10.5 *tauGFP* embryos that were cultured on membranes, the outgrowing axons showed normal growth patterns and no innervation of normally avoided tissue regions in the forelimb. This result allowed us to conclude that not only the short and long range guidance cues, but also the trophic factors which are needed for a proper pathfinding, were still provided by the limb tissue itself. Since the slices are easily accessible, these cultures provide a powerful system to address questions related to axon guidance (Tucker et al., 2001). Several approaches to target developmental processes would be easy to perform: application of beads soaked with a protein of preference, transplantation of transfected cells or tissue grafts, or addition of chemical compounds into the culture medium.

Slice cultures of older embryos (E11.5-E12.5) revealed a less consistent outgrowth, most likely due to the complex three-dimensional arrangement of cords and rami of the brachial plexus which is therefore at a higher risk to be dissected during the slicing procedure. A way to increase the viability might be the preparation of thicker slices.

One critical parameter for maintenance of short-term growth at each embryonic age was temperature. Even short drops in temperature of 5-10 degrees centigrade reduced the successful outgrowth tremendously.

4.1.3 The rate of spinal nerve outgrowth in transverse slices

Spinal nerves, arising from the fifth cervical to the first thoracic segment, form three trunks that separate and refasciculate, thereby establishing the brachial plexus, to finally establish the nerves innervating the forelimb. As known from experiments on chick hindlimbs, motor and sensory axons experience a waiting period at the base of the limb before invading the limb itself (Tosney and Landmesser 1985; Wang and Scott 2000). To test if a similar mechanism occurs during the pathfinding of nerves into the mouse forelimb, nerve endings of several slices achieved from littermates were imaged at regular time intervals. Measuring the outgrowth of nerve endings revealed a continuous outgrowth for most of the nerves, but didn't display similar outgrowth rates. This might be due to the fact that although only slices of littermates were compared to each other, significant differences in their developmental stages existed. Another cause for this diversity could lie in the intrinsic developmental pattern of different spinal cord segments that are sending nerve fibres into the forelimb.

4.1.4 Imaging nerve outgrowth in sagittal sections

The continuous outgrowth of nerves in transverse sections proved the slice culture system a valuable tool to follow axonal pathfinding. Since the nerves displayed by the slices depend on the section plane, and represent only a subset of the ones innervating the forelimb, an alternative approach to document the formation of the brachial plexus was to use sagittal slices. Embryos were dissected and embedded as for transverse slices, but then glued in a different orientation on the vibratome chuck. Several trials had to be performed to find the correct angle for mounting the embryo. Also a major portion of the spinal cord needed to be present in the slices itself. After increasing the thickness of the slices up to 500 µm several sections displayed continuous outgrowth during culture periods of 24-36 hours.

Although the spinal nerves showed a continuous outgrowth and the innervation patterns resembled the endogenous ones, the outgrowth was considerably slower compared to the innervation pattern with whole mount stainings from E11.5 embryos. This could partially be explained as a delay which results from the dissection and cutting in icecold 1x PBS and 1x HBSS. Another critical point is the integrity of the neural tube, since both the motor neurons sitting in the mantle zone and the sensory projections entering through the dorsal entry zone depend on it. In conclusion, we recommend the cultures system using transverse sections. They are easily established and the axonal outgrowth of the left and right spinal nerves can be compared.

4.1.5 Development of non-neural tissue within cultured slices

Between E10.5 and E11.5, several important changes occur in the development of the limb bud itself. Analyzing slices of E10.5 embryos that were cultured for 24 hours and comparing them to slices generated of E11.5 old embryos, a normal development of non-neural tissues in the forelimb bud could be shown.

SEM revealed that aside from some anomalous cell growth out of the dorsal neural tube and a formation of a fissure in the dorsal-most aspect of the neural tube in a proportion of slices, the tissue appeared morphologically normal during and after the culture period. The surface of the slices was not overgrown with epidermal cells or covered by cell debris and most importantly, periderm cells developed at the distal forelimb.

The staining for the myogenic marker MyoD in our cultured slices resembled the pattern that was observed in slices prepared of E11.5 old embryos. However, the size of the forelimbs in cultured slices is significantly smaller compared to limb buds of E11.5 embryos. This might be due to the small fraction of the AER each slice contains, since experimental removal of the AER was shown to result in a truncation of the distal portion of the limb (Fernandez-Teran and Ros 2008).

FACS and apoptosis analysis demonstrated a relative low mortality rate of both neurons and non-neuronal cells, for FACS analysis even after 48 hours in culture.

Tthe slice culture system presented here obviously allows for a faithful reproduction of the initial steps of innervation of the forelimb by neurons of the spinal cord and DRG, and thus provides a powerful model system to investigate spinal nerve development *in situ*.

4.2 Advantages for imaging using the M22 mouse line

To increase the amount of slices in which nerve outgrowth can be imaged even if nerves reach a depth of more than 200 µm in the tissue, a mouse line (M22-tauGFP) with a higher expression level of GFP was established. The new colony was set up to achieve animals with a maximum amount of EGFP expression.

Comparing the staining for anti-TuJI and anti-GFP revealed a complete colocalisation of the two proteins, demonstrating a highly specific EGFP expression pattern in the central and peripheral nervous system of E10.5 M22-tauGFP mouse embryos. Using slices of these embryos, it became easier to follow and to document nerve outgrowth even at low magnifications. The innervation pattern of the forelimb revealed in these slices was similar to that observed in the slices of the *tauGFP* mice.

According to the stronger neuronal EGFP signal, this model offered us the possibility to image single nerve endings and growth cones and to study the behaviour of growth cones and their interaction with the environment which has not been performed so far *in vivo*. Combining our high GFP-expressing M22-tauGFP mouse line with another transgenic line expressing a growth cone marker labeled with a different fluorophore could be helpful to answer very specific questions about axon guidance. Also crossing M22-tauGFP to a mouse line expressing yellow or red fluorescent proteins specifically in a subset of neurons (sensory or motor neurons) would

enable to distinguish between different populations of neurons and their corresponding axons and to address their outgrowth rates and response to guidance cues. The signal of the M22-tauGFP mouse line might even be strong enough to use it at an inverted confocal microscope, offering distinct imaging in several tissue layers.

4.3 Application of the slice culture system for the analysis of mutant mouse lines

Most of the data originating from transgenic lines that show defects in neuronal outgrowth and guidance was generated in *in vitro* assays or by histochemical techniques at defined time intervals. Despite the amount of results gained from these cultures, one would like to observe and manipulate spinal nerve outgrowth as it occurs *in vivo*. To test if our system provided a valuable tool for such an analysis, we crossed mice of the *tauGFP* line to mice lacking the gene encoding the chemorepulsive secreted protein Sema3A.

4.3.1 Imaging neuronal outgrowth in the *tauSEM*$^{-/-}$ mouse line

The *tauSEM* mouse line allowed us to reproduce and confirm two key features in the slice culture system which were found in Sema3A mutant embryos. First, a precocious outgrowth of spinal nerves, as described by Huber et al., (2005) and second, aberrant nerve projections deriving directly from the DRG and aberrant branches from the spinal nerves as reported by Taniguchi and coworkers as well as by White and Behar (Behar et al., 1996; Taniguchi et al., 1997). The observed resemblance of the branching pattern of spinal nerves between control and the *tauSEM*$^{-/-}$ embryos after a culture period of 25-37 hours might reveal the beginning of the so-called "self-correction" process that was described to occur between initial outgrowth and birth (White and Behar 2000).

Furthermore, our slice culture system lead to the detection of cells located laterally to the DRGs that had not been described before. From these data, we conclude that our culture system offers the possibility to analyze molecular mechanisms important for axonal outgrowth and pathfinding, and those crucial for cell migration.

4.3.2 Characterisation of ectopic cells in *tauSEM*$^{-/-}$ mouse embryos

Two possible mechanisms were considered to explain the ectopic localization of precursor cells detected in *tauSEM*$^{-/-}$animals. One could be that postmitotic neurons follow aberrant projections from their original location which would explain why we detected these cells only in the vicinity of fascicles. Another explanation could be that neural crest cells are migrating into tissue areas that became permissive according to the lack of Sema3A and eventually differentiate into sensory and sympathetic neurons.

Since all ectopic cells expressed GFP and were therefore presumptive postmitotic neurons we started with their characterisation employing neuronal markers. Stainings using anti-TH and anti-Brn3a each labelled a subset of ectopic GFP positive cells and revealed two distinct populations which are neural crest cell derivatives, originating from the sensory and smpathetic lineage that undertook incorrect migration pathways. To characterize their origin further stainings applying neural crest markers such as p75 and Sox10 are needed to determine the spatiotemporal role of Sema3A on neural crest migration at the forelimb level including also stainings on sections from younger embryos.

According to previously published investigations Sema6A embryos lacking the signal transduction reveal motor neurons that stream out of the spinal cord (Mauti et al., 2007). This effect was described to be dependent on boundary cap cells, a population of cells developing from neural crest cells. Additionally oligodendrocyte precursor cells were described to be dependent on Sema3A (Klambt 2009), as well as a Sema3A-responsiveness of migrating trunk neural crest cells was shown (Schwarz et al., 2009; Schwarz et al., 2009). Our observations provide evidence that ectopic neural crest derivatives follow the abnormal branching patterns of spinal nerves in *tauSEM*$^{-/-}$animals.

It remains to be shown if Sema3A only provides a guidance cue that is involved in the establishment of a proper metameric peripheral nervous system or even provides signals that are essential for neural crest cell differentiation.

4.4 Neural crest cells

Neural crest cells are a transient, multipotent, and migratory population. Since their first description by His in 1868 they have fascinated developmental and evolutionary biologists, providing a unique paradigm with which to investigate principle developmental mechanisms such as morphogenetic induction, cell migration, and fate determination (Crane and Trainor 2006).

In order to become migratory they need to undergo an epithelial mesenchymal transition (EMT) which takes place within the dorsal neural epithelium (Thiery et al., 2009). Trunk neural crest cells migrate, controlled by various signals present in the environment through the rostral half of each somite (Gammill and Roffers-Agarwal 2010).

To test if Sema3A is one of these signals, neural tube explant cultures were prepared and cultivated for 20-48 hours. As described for chick neural crest cultures, application of Sema3A (1µg/ml) for 30 min lead to morphological changes, including cell rounding that correlated with a disruption of the actin meshwork (Eickholt et al., 1999). Reproducing a modification of published protocols with neural tubes of E9.0 to 9.75 mouse embryos (Ito and Takeuchi 1984; Stemple and Anderson 1992; Greenwood et al., 1999), we achieved cultures that revealed neural crest cell migration. However, adding Sema3A to these cultures did not show significant changes in cell morphology, nor did employing time-lapse experiments using a Biostation allow us to detect any changes in the actin cytoskeleton (filopodia retraction), that seemed to be specific to the addition of Sema3A. In contrast DRG cultures used as controls revealed a biological activity of Sema3A, applying medium that was produced by Sema3A transfected HEK293 cells.

If the differences in responsiveness to Sema3A are based on the developmental stage of the neural crest cells, on the culture methods itself, or on the distinct species remains to be investigated.

4.5 Future research

Neural crest cell guidance in the trunk region was known to be regulated by Eph/ephrin and Sema3F signaling (Gammill et al., 2006; Davy and Soriano 2007). As we and others could show also Sema3A signaling is important for the correct migration pathways of neural crest cells. However, a possible spatial and temporal interaction of these pathways has not been analysed previously.

In order to gain insight and to improve our knowledge about the receptor complexes the Sema3A signaling is dependent on in migrating neural crest cells, and to investigate if Sema3A responsive neural crest cells might also express ephrin receptors, *in situ* hybridization on vibratome sections was started. Probes for ephrinB1, ephrinB2, EphA4, EphB1, EphB2, Nrp1, Nrp2 as well as plexinA1, plexinA2, plexinA3 and plexinA4 were already generated but still need to be applied successfully on tauGFP or *tauSEM*$^{+/-}$ and *tauSEM*$^{-/-}$ tissue samples.

References

Adams, R. H., M. Lohrum, et al. (1997). "The chemorepulsive activity of secreted semaphorins is regulated by furin-dependent proteolytic processing." EMBO J 16(20): 6077-6086.

Anderson, C. N., K. Ohta, et al. (2003). "Molecular analysis of axon repulsion by the notochord." Development 130(6): 1123-1133.

Bagnard, D., C. Vaillant, et al. (2001). "Semaphorin 3A-vascular endothelial growth factor-165 balance mediates migration and apoptosis of neural progenitor cells by the recruitment of shared receptor." J Neurosci 21(10): 3332-3341.

Behar, O., J. A. Golden, et al. (1996). "Semaphorin III is needed for normal patterning and growth of nerves, bones and heart." Nature 383(6600): 525-528.

Belmadani, A., P. B. Tran, et al. (2005). "The chemokine stromal cell-derived factor-1 regulates the migration of sensory neuron progenitors." J Neurosci 25(16): 3995-4003.

Brachmann, I. (2005). Analyse des Zentralen und Peripheren Nervensystems der Mausmutantenlinie tauGFP währen der Embryonalentwicklung. Fakultät für Biowissenschaften. Heidelberg, University of Heidelberg. Diplom Biologie.

Brachmann, I., V. C. Jakubick, et al. (2007). "A simple slice culture system for the imaging of nerve development in embryonic mouse." Dev Dyn 236(12): 3514-3523.

Brown, C. B., L. Feiner, et al. (2001). "PlexinA2 and semaphorin signaling during cardiac neural crest development." Development 128(16): 3071-3080.

Castellani, V. (2002). "The function of neuropilin/L1 complex." Adv Exp Med Biol 515: 91-102.

Castellani, V., A. Chedotal, et al. (2000). "Analysis of the L1-deficient mouse phenotype reveals cross-talk between Sema3A and L1 signaling pathways in axonal guidance." Neuron 27(2): 237-249.

Castellani, V., E. De Angelis, et al. (2002). "Cis and trans interactions of L1 with neuropilin-1 control axonal responses to semaphorin 3A." EMBO J 21(23): 6348-6357.

Committee, S. N. (1999). Unified nomenclature for the semaphorins/collapsins. Semaphorin Nomenclature Committee. Cell. 97: 551-552.

Crane, J. F. and P. A. Trainor (2006). "Neural crest stem and progenitor cells." Annu Rev Cell Dev Biol 22: 267-286.

Davy, A. and P. Soriano (2007). "Ephrin-B2 forward signaling regulates somite patterning and neural crest cell development." Dev Biol 304(1): 182-193.

Debby-Brafman, A., T. Burstyn-Cohen, et al. (1999). "F-Spondin, expressed in somite regions avoided by neural crest cells, mediates inhibition of distinct somite domains to neural crest migration." Neuron 22(3): 475-488.

Dickson, B. J. (2002). "Molecular mechanisms of axon guidance." Science 298(5600): 1959-1964.

Dutt, S., M. Kleber, et al. (2006). "Versican V0 and V1 guide migratory neural crest cells." J Biol Chem 281(17): 12123-12131.

Dutt, S., M. Matasci, et al. (2006). "Guidance of neural crest cell migration: the inhibitory function of the chondroitin sulfate proteoglycan, versican." ScientificWorldJournal 6: 1114-1117.

Eastwood, S. L., A. J. Law, et al. (2003). "The axonal chemorepellant semaphorin 3A is increased in the cerebellum in schizophrenia and may contribute to its synaptic pathology." Mol Psychiatry 8(2): 148-155.

Eickholt, B. J., S. L. Mackenzie, et al. (1999). "Evidence for collapsin-1 functioning in the control of neural crest migration in both trunk and hindbrain regions." Development 126(10): 2181-2189.

Erickson, C. A. and J. A. Weston (1983). "An SEM analysis of neural crest migration in the mouse." J Embryol Exp Morphol 74: 97-118.

Fedtsova, N. G. and E. E. Turner (1995). "Brn-3.0 expression identifies early post-mitotic CNS neurons and sensory neural precursors." Mech Dev 53(3): 291-304.

Feiner, L., A. L. Webber, et al. (2001). "Targeted disruption of semaphorin 3C leads to persistent truncus arteriosus and aortic arch interruption." Development 128(16): 3061-3070.

Fernandez-Teran, M. and M. A. Ros (2008). "The Apical Ectodermal Ridge: morphological aspects and signaling pathways." Int J Dev Biol 52(7): 857-871.

Fernandez-Teran, M. A., J. R. Hinchliffe, et al. (2006). "Birth and death of cells in limb development: a mapping study." Dev Dyn 235(9): 2521-2537.

Gammill, L. S., C. Gonzalez, et al. (2006). "Guidance of trunk neural crest migration requires neuropilin 2/semaphorin 3F signaling." Development 133(1): 99-106.

Gammill, L. S. and J. Roffers-Agarwal (2010). "Division of labor during trunk neural crest development." Dev Biol 344(2): 555-565.

Gilbert, S. F. (2010). Developmental Biology, Sinauer Associates.

Greenwood, A. L., E. E. Turner, et al. (1999). "Identification of dividing, determined sensory neuron precursors in the mammalian neural crest." Development 126(16): 3545-3559.

Gu, C., E. R. Rodriguez, et al. (2003). "Neuropilin-1 conveys semaphorin and VEGF signaling during neural and cardiovascular development." Dev Cell 5(1): 45-57.

Guttmann-Raviv, N., N. Shraga-Heled, et al. (2007). "Semaphorin-3A and semaphorin-3F work together to repel endothelial cells and to inhibit their survival by induction of apoptosis." J Biol Chem 282(36): 26294-26305.

Hall, B. K. (2009). The Neural Crest and Neural Crest Cells in Vertebrate Development and Evolution, Springer.

Halloran, M. C. and M. A. Wolman (2006). "Repulsion or adhesion: receptors make the call." Curr Opin Cell Biol 18(5): 533-540.

He, Z. and M. Tessier-Lavigne (1997). "Neuropilin is a receptor for the axonal chemorepellent Semaphorin III." Cell 90(4): 739-751.

Hirsch, E., L. J. Hu, et al. (1999). "Distribution of semaphorin IV in adult human brain." Brain Res 823(1-2): 67-79.

Hollyday, M. and M. Morgan-Carr (1995). "Chick wing innervation. II. Morphology of motor and sensory axons and their growth cones during early development." J Comp Neurol 357(2): 254-271.

Hou, S. T., A. Keklikian, et al. (2008). "Sustained up-regulation of semaphorin 3A, Neuropilin1, and doublecortin expression in ischemic mouse brain during long-term recovery." Biochem Biophys Res Commun 367(1): 109-115.

Huber, A. B., A. Kania, et al. (2005). "Distinct roles for secreted semaphorin signaling in spinal motor axon guidance." Neuron 48(6): 949-964.

Huber, A. B., A. L. Kolodkin, et al. (2003). "Signaling at the growth cone: ligand-receptor complexes and the control of axon growth and guidance." Annu Rev Neurosci 26: 509-563.

Imai, T., T. Yamazaki, et al. (2009). "Pre-target axon sorting establishes the neural map topography." Science 325(5940): 585-590.

Ito, K. and T. Takeuchi (1984). "The differentiation in vitro of the neural crest cells of the mouse embryo." J Embryol Exp Morphol 84: 49-62.

Ito, T., M. Kagoshima, et al. (2000). "Repulsive axon guidance molecule Sema3A inhibits branching morphogenesis of fetal mouse lung." Mech Dev 97(1-2): 35-45.

Kagoshima, M. and T. Ito (2001). "Diverse gene expression and function of semaphorins in developing lung: positive and negative regulatory roles of semaphorins in lung branching morphogenesis." Genes Cells 6(6): 559-571.

Kasemeier-Kulesa, J. C., R. McLennan, et al. (2010). "CXCR4 controls ventral migration of sympathetic precursor cells." J Neurosci 30(39): 13078-13088.

Kaufmann, M. H. (2001). The Atlas of Mouse Development, Academic Press.

Kawasaki, T., Y. Bekku, et al. (2002). "Requirement of neuropilin 1-mediated Sema3A signals in patterning of the sympathetic nervous system." Development 129(3): 671-680.

Khare, N., N. Fascetti, et al. (2000). "Expression patterns of two new members of the Semaphorin family in Drosophila suggest early functions during embryogenesis." Mech Dev 91(1-2): 393-397.

Kitsukawa, T., M. Shimizu, et al. (1997). "Neuropilin-semaphorin III/D-mediated chemorepulsive signals play a crucial role in peripheral nerve projection in mice." Neuron 19(5): 995-1005.

Klambt, C. (2009). "Modes and regulation of glial migration in vertebrates and invertebrates." Nat Rev Neurosci 10(11): 769-779.

Kolodkin, A. L., D. V. Levengood, et al. (1997). "Neuropilin is a semaphorin III receptor." Cell 90(4): 753-762.

Kolodkin, A. L., D. J. Matthes, et al. (1993). "The semaphorin genes encode a family of transmembrane and secreted growth cone guidance molecules." Cell 75(7): 1389-1399.

Kolodkin, A. L., D. J. Matthes, et al. (1992). "Fasciclin IV: sequence, expression, and function during growth cone guidance in the grasshopper embryo." Neuron 9(5): 831-845.

Kruger, R. P., J. Aurandt, et al. (2005). "Semaphorins command cells to move." Nat Rev Mol Cell Biol 6(10): 789-800.

Kulesa, P. M. and L. S. Gammill (2010). "Neural crest migration: patterns, phases and signals." Dev Biol 344(2): 566-568.

Law, C. O., R. J. Kirby, et al. (2008). "The neural adhesion molecule TAG-1 modulates responses of sensory axons to diffusible guidance signals." Development 135(14): 2361-2371.

Le Douarin, N. M. a. K., K (2009). The Neural Crest, Cambridge University Press.

Lepelletier, Y., S. Smaniotto, et al. (2007). "Control of human thymocyte migration by Neuropilin-1/Semaphorin-3A-mediated interactions." Proc Natl Acad Sci U S A 104(13): 5545-5550.

Loes, S., K. Luukko, et al. (2003). "Developmentally regulated expression of Netrin-1 and -3 in the embryonic mouse molar tooth germ." Dev Dyn 227(4): 573-577.

Luo, Y., D. Raible, et al. (1993). "Collapsin: a protein in brain that induces the collapse and paralysis of neuronal growth cones." Cell 75(2): 217-227.

Marin, O., A. Yaron, et al. (2001). "Sorting of striatal and cortical interneurons regulated by semaphorin-neuropilin interactions." Science 293(5531): 872-875.

Martin, P. (1990). "Tissue patterning in the developing mouse limb." Int J Dev Biol 34(3): 323-336.

Masuda, T., H. Tsuji, et al. (2003). "Differential non-target-derived repulsive signals play a critical role in shaping initial axonal growth of dorsal root ganglion neurons." Dev Biol 254(2): 289-302.

Mauti, O., E. Domanitskaya, et al. (2007). "Semaphorin6A acts as a gate keeper between the central and the peripheral nervous system." Neural Dev 2: 28.

Messersmith, E. K., E. D. Leonardo, et al. (1995). "Semaphorin III can function as a selective chemorepellent to pattern sensory projections in the spinal cord." Neuron 14(5): 949-959.

Milaire, J. and J. Mulnard (1984). "Histogenesis in 11-day mouse embryo limb buds explanted in organ culture." J Exp Zool 232(2): 359-377.

Miyamichi, K. and L. Luo (2009). "Neuroscience. Brain wiring by presorting axons." Science 325(5940): 544-545.

Moret, F., C. Renaudot, et al. (2007). "Semaphorin and neuropilin co-expression in motoneurons sets axon sensitivity to environmental semaphorin sources during motor axon pathfinding." Development 134(24): 4491-4501.

Muneoka, K., N. Wanek, et al. (1989). "Mammalian limb bud development: in situ fate maps of early hindlimb buds." J Exp Zool 249(1): 50-54.

Nakamura, F., R. G. Kalb, et al. (2000). "Molecular basis of semaphorin-mediated axon guidance." J Neurobiol 44(2): 219-229.

Nakamura, H. and M. Yasuda (1979). "An electron microscopic study of periderm cell development in mouse limb buds." Anat Embryol (Berl) 157(2): 121-132.

Oakley, R. A., C. J. Lasky, et al. (1994). "Glycoconjugates mark a transient barrier to neural crest migration in the chicken embryo." Development 120(1): 103-114.

Oakley, R. A. and K. W. Tosney (1991). "Peanut agglutinin and chondroitin-6-sulfate are molecular markers for tissues that act as barriers to axon advance in the avian embryo." Dev Biol 147(1): 187-206.

Pasterkamp, R. J. and A. L. Kolodkin (2003). "Semaphorin junction: making tracks toward neural connectivity." Curr Opin Neurobiol 13(1): 79-89.

Pasterkamp, R. J. and J. Verhaagen (2006). "Semaphorins in axon regeneration: developmental guidance molecules gone wrong?" Philos Trans R Soc Lond B Biol Sci 361(1473): 1499-1511.

Puschel, A. W. (1996). "The semaphorins: a family of axonal guidance molecules?" Eur J Neurosci 8(7): 1317-1321.

Puschel, A. W., R. H. Adams, et al. (1995). "Murine semaphorin D/collapsin is a member of a diverse gene family and creates domains inhibitory for axonal extension." Neuron 14(5): 941-948.

Puschel, A. W., R. H. Adams, et al. (1996). "The sensory innervation of the mouse spinal cord may be patterned by differential expression of and differential responsiveness to semaphorins." Mol Cell Neurosci 7(5): 419-431.

Ranscht, B. and M. Bronner-Fraser (1991). "T-cadherin expression alternates with migrating neural crest cells in the trunk of the avian embryo." Development 111(1): 15-22.

Raper, J. and C. Mason (2010). "Cellular strategies of axonal pathfinding." Cold Spring Harb Perspect Biol 2(9): a001933.

Ring, C., J. Hassell, et al. (1996). "Expression pattern of collagen IX and potential role in the segmentation of the peripheral nervous system." Dev Biol 180(1): 41-53.

Rohm, B., A. Ottemeyer, et al. (2000). "Plexin/neuropilin complexes mediate repulsion by the axonal guidance signal semaphorin 3A." Mech Dev 93(1-2): 95-104.

Roth, L., E. Koncina, et al. (2009). "The many faces of semaphorins: from development to pathology." Cell Mol Life Sci 66(4): 649-666.

Sauka-Spengler, T. and M. Bronner-Fraser (2008). "A gene regulatory network orchestrates neural crest formation." Nat Rev Mol Cell Biol 9(7): 557-568.

Schachner, M. (1991). "Cell surface recognition and neuron-glia interactions." Ann N Y Acad Sci 633: 105-112.

Schwarz, Q., C. Gu, et al. (2004). "Vascular endothelial growth factor controls neuronal migration and cooperates with Sema3A to pattern distinct compartments of the facial nerve." Genes Dev 18(22): 2822-2834.

Schwarz, Q., C. H. Maden, et al. (2009). "Neuropilin-mediated neural crest cell guidance is essential to organise sensory neurons into segmented dorsal root ganglia." Development 136(11): 1785-1789.

Schwarz, Q., C. H. Maden, et al. (2009). "Neuropilin 1 signaling guides neural crest cells to coordinate pathway choice with cell specification." Proc Natl Acad Sci U S A 106(15): 6164-6169.

Schwarz, Q., J. M. Vieira, et al. (2008). "Neuropilin 1 and 2 control cranial gangliogenesis and axon guidance through neural crest cells." Development 135(9): 1605-1613.

Serbedzija, G. N., S. E. Fraser, et al. (1990). "Pathways of trunk neural crest cell migration in the mouse embryo as revealed by vital dye labelling." Development 108(4): 605-612.

Shepherd, I. T., Y. Luo, et al. (1997). "A sensory axon repellent secreted from ventral spinal cord explants is neutralized by antibodies raised against collapsin-1." Development 124(7): 1377-1385.

Slack, J. M. W. (2006). Essential developmental biology, Blackwell publishing.

Stemple, D. L. and D. J. Anderson (1992). "Isolation of a stem cell for neurons and glia from the mammalian neural crest." Cell 71(6): 973-985.

Suto, F., K. Ito, et al. (2005). "Plexin-a4 mediates axon-repulsive activities of both secreted and transmembrane semaphorins and plays roles in nerve fiber guidance." J Neurosci 25(14): 3628-3637.

Takahashi, T. and S. M. Strittmatter (2001). "Plexina1 autoinhibition by the plexin sema domain." Neuron 29(2): 429-439.

Taniguchi, M., S. Yuasa, et al. (1997). "Disruption of semaphorin III/D gene causes severe abnormality in peripheral nerve projection." Neuron 19(3): 519-530.

Tessier-Lavigne, M. and C. S. Goodman (1996). "The molecular biology of axon guidance." Science 274(5290): 1123-1133.

Thiery, J. P., H. Acloque, et al. (2009). "Epithelial-mesenchymal transitions in development and disease." Cell 139(5): 871-890.

Tosney, K. W. and L. T. Landmesser (1985). "Development of the major pathways for neurite outgrowth in the chick hindlimb." Dev Biol 109(1): 193-214.

Towers, M. and C. Tickle (2009). "Generation of pattern and form in the developing limb." Int J Dev Biol 53(5-6): 805-812.

Toyofuku, T., J. Yoshida, et al. (2005). "FARP2 triggers signals for Sema3A-mediated axonal repulsion." Nat Neurosci 8(12): 1712-1719.

Tran, T. S., A. L. Kolodkin, et al. (2007). "Semaphorin regulation of cellular morphology." Annu Rev Cell Dev Biol 23: 263-292.

Tucker, K. L., M. Meyer, et al. (2001). "Neurotrophins are required for nerve growth during development." Nat Neurosci 4(1): 29-37.

Varela-Echavarria, A., A. Tucker, et al. (1997). "Motor axon subpopulations respond differentially to the chemorepellents netrin-1 and semaphorin D." Neuron 18(2): 193-207.

Villegas, G. and A. Tufro (2002). "Ontogeny of semaphorins 3A and 3F and their receptors neuropilins 1 and 2 in the kidney." Gene Expr Patterns 2(1-2): 151-155.

Wang, G. and S. A. Scott (2000). "The "waiting period" of sensory and motor axons in early chick hindlimb: its role in axon pathfinding and neuronal maturation." J Neurosci 20(14): 5358-5366.

Wang, H. U. and D. J. Anderson (1997). "Eph family transmembrane ligands can mediate repulsive guidance of trunk neural crest migration and motor axon outgrowth." Neuron 18(3): 383-396.

White, F. A. and O. Behar (2000). "The development and subsequent elimination of aberrant peripheral axon projections in Semaphorin3A null mutant mice." Dev Biol 225(1): 79-86.

Williams, A., G. Piaton, et al. (2007). "Semaphorin 3A and 3F: key players in myelin repair in multiple sclerosis?" Brain 130(Pt 10): 2554-2565.

Winberg, M. L., L. Tamagnone, et al. (2001). "The transmembrane protein Off-track associates with Plexins and functions downstream of Semaphorin signaling during axon guidance." Neuron 32(1): 53-62.

Wright, D. E., F. A. White, et al. (1995). "The guidance molecule semaphorin III is expressed in regions of spinal cord and periphery avoided by growing sensory axons." J Comp Neurol 361(2): 321-333.

Yamamoto, M., K. Suzuki, et al. (2008). "Plexin-A4 negatively regulates T lymphocyte responses." Int Immunol 20(3): 413-420.

Yaron, A., P. H. Huang, et al. (2005). "Differential requirement for Plexin-A3 and -A4 in mediating responses of sensory and sympathetic neurons to distinct class 3 Semaphorins." Neuron 45(4): 513-523.

Yaron, A. and B. Zheng (2007). "Navigating their way to the clinic: emerging roles for axon guidance molecules in neurological disorders and injury." Dev Neurobiol 67(9): 1216-1231.

Yazdani, U. and J. R. Terman (2006). "The semaphorins." Genome Biol 7(3): 211.

Zeller, R., J. Lopez-Rios, et al. (2009). "Vertebrate limb bud development: moving towards integrative analysis of organogenesis." Nat Rev Genet 10(12): 845-858.

Zhou, Y., R. A. Gunput, et al. (2008). "Semaphorin signaling: progress made and promises ahead." Trends Biochem Sci 33(4): 161-170.

Zimmer, G., S. M. Schanuel, et al. (2010). "Chondroitin sulfate acts in concert with semaphorin 3A to guide tangential migration of cortical interneurons in the ventral telencephalon." Cereb Cortex 20(10): 2411-2422.

List of Abbreviations

%	per cent
°C	degree Celsius
ab	antibody
bp	base pair(s)
BDNF	brain derived neurotrophic factor
BSA	bovine serum albumin
DMEM	“Dulbecco’s Modified Eagle Medium”
DNA	deoxyribonucleic acid
DRG	dorsal root ganglion
EGFP	enhanced green fluorescent protein
EMT	epithelial mesenchymal transition
FACS	fluorescent activated cell sorting
FBS	fetal bovine serum
GFP	green fluorescent protein
HBSS	Hanks balanced salt solution
Hepes	(N-2-Hydroxyethyl)-piperazin-N’-(2-ethansulfonic acid)
HRP	horseradish peroxidase
h	hours
kb	kilobase
KO	knockout
l	liter
LB	Luria-Bertani medium
LMP	low melting point
µ	micrometer
m	millimeter
M	molar
Mapt	microtubule-associated protein tau
MEF	mouse embryonic fibroblast
ml	milliliter
NCS	newborn calf serum

NGF	nerve growth factor
NGS	normal goat serum
NT3	neurotrophin 3
PBS	phosphate buffered saline
PCR	polymerase chain reaction
PEI	polyethyleneimine
PFA	paraformaldehyde
P/S	penicillin/streptomycin
SDS	sodiumdodecylsulfate
Sema3A	semaphorin3A / collapsin-1
$Sema3A^{-/-}$	semaphorin deficient mice
tauGFP	tau deficient and GFP expressing mice
$tauSEM^{+/-}$	tau deficient and GFP expressing mice, additionally heterozygous deficient for Sema3A
$tauSEM^{-/-}$	tau deficient and GFP expressing mice, additionally homozygous deficient for Sema3A
UV	ultraviolet
WT	wild type

Publications

Brachmann, I., Jakubick, V.C., Shakèd, M., Unsicker, K., Tucker, K.L. (2007)
A simple slice culture system for the imaging of nerve development in embryonic mouse.
Developmental Dynamics **236** (12): 3514 – 3523.

Brachmann, I., Tucker, K.L.
Organotypic slice culture of GFP-expressing mouse embryos for real-time imaging of peripheral nerve outgrowth.
Journal of Visualized Experiments
In press

Brachmann, I., Herzer, S., Tucker, K.L.
„Role of Sema3A in neural crest development and spinal nerve outgrowth."
Manuscript in preparation

Acknowledgements

This PhD thesis was performed in the lab of Dr. Kerry L. Tucker within the Interdisciplinary Center for Neurosciences (IZN) at the Institute of Anatomy and Cell Biology of the University of Heidelberg. The project belonged to the Teilprojekt B7 of the Sonderforschungsbereich 488 of the German Research Foundation (DFG) “Molecular and cellular bases of neural development”.

I would like to thank Dr. Kerry L. Tucker for giving me the opportunity to work in his lab and offering me this interesting project. His support and encouragement to be critical and to work self dependent were essential and very helpful performing this thesis.

I am deeply grateful to Prof. Karin Gorgas for mentoring, critique and scientific discussions. Sharing her attitude to work precise and giving perspectives allowed a constant positive view.

I thank Maya Shakèd-Rabi, Vera Jakubick-Warnecke, and Silke Herzer for their help to perform experiments and aquire images.

My thanks also goes to Maya, Hitomi, Michal, Thomas, Raphael, Dorde, Marc, Dmitry, Nina, Mariya, Christoph, Daniel and Francisco for the nice and productive atmosphere at the Department and the pleasant and joyful events besides work, as the cherry blossom picnic, a bike tour to Freinsheim, the beach volleyball summer sessions, a barbecue in February and further sports and cooking activities.
Special thanks to Silke for sharing the interest in this project and being encouraged enough to perform a bachelor thesis depending on mice. It was my pleasure to join forces with her and Hannah, and to keep the exercises on Tuesday evenings.

This thesis would not have been possible without the constant support of Olav, Magdalena, Friedhelm, Ines, Holger and Faina. Thank you for your love, sympathy and respect for this work and the changes that came along with it.

Hiermit erkläre ich, dass ich die vorliegende Dissertation selbständig verfasst und mich dabei keiner anderen, als der von mir ausdrücklich bezeichneten Quellen bedient habe.

Heidelberg, den 14. Oktober 2010 ……..

Isabel Brachmann